MOX-Report No. 08/2023

Discrete tensor product BGG sequences: splines and finite elements

Bonizzoni, F.; Hu, K.; Kanschat, G.; Sap, D.

MOX, Dipartimento di Matematica
Politecnico di Milano, Via Bonardi 9 - 20133 Milano (Italy)

mox-dmat@polimi.it https://mox.polimi.it

DISCRETE TENSOR PRODUCT BGG SEQUENCES: SPLINES AND FINITE ELEMENTS

FRANCESCA BONIZZONI, KAIBO HU, GUIDO KANSCHAT, AND DUYGU SAP

Abstract. In this paper, we provide a systematic discretization of the Bernstein-Gelfand-Gelfand (BGG) diagrams and complexes over cubical meshes of arbitrary dimension via the use of tensor-product structures of one-dimensional piecewise-polynomial spaces, such as spline and finite element spaces. We demonstrate the construction of the Hessian, the elasticity, and div div complexes as examples for our construction.

Differential complexes encode key algebraic structures in analysis and computation for partial differential equations. In addition to the de-Rham complex with applications in electromagnetism, other complexes, such as the elasticity (Kröner, Calabi, Riemannian deformation) complex, are drawing attention for problems in areas such as geometry, general relativity and continuum mechanics [1, 4, 6, 10, 44, 45]. These complexes are special cases of the so-called Bernstein-Gelfand-Gelfand (BGG) sequences [6, 10, 16, 17, 18]. Recently, a systematic study of the construction of BGG complexes and their properties was given in [10] with generalizations in [16] (see also the results therein for results for individual complexes).

In the framework of the finite element exterior calculus (FEEC) [4, 7, 9], there has been a systematic discretization of the de-Rham complex in any dimension for any form and polynomial degree, as summarized in the finite element periodic table [11] (although questions like regular complexes and

1991 *Mathematics Subject Classification.* 65N99; 41A15, 41A63, 65N30.

Key words and phrases. Bernstein-Gelfand-Gelfand sequence, tensor product, splines, finite elements.

FB acknowledges support from the HGS MathComp through the Distinguished Romberg Guest Professorship Program. Moreover, FB is member of the INdAM Research group GNCS and her work was part of a project that has received funding from the European Research Council ERC under the European Union's Horizon 2020 research and innovation program (Grant agreement No. 865751).

KH was supported by a Hooke Research Fellowship and a Royal Society University Research Fellowship (URF\R1\221398) .

GK was supported by the Deutsche Forschungsgemeinschaft (DFG, German Research Foundation) under Germany's Excellence Strategy EXC 2181/1 - 390900948 (the Heidelberg STRUCTURES Excellence Cluster).

DS was supported by the Engineering and Physical Sciences Research Council (EPSRC) grants EP/S005072/1 and EP/R029423/1 for the projects ASiMoV (Advanced Simulation and Modelling of Virtual Systems) and the PRISM (Platform for Research in Simulation Methods), respectively.

The authors would like to thank Espen Sande for helpful discussions.

computational issues are still active and important research topics). The Hellinger-Reissner formulation of linear elasticity involves the last two spaces of the elasticity complex [4]. Since the seminal work on conforming finite elements on triangular meshes by Arnold and Winther [12], there has been a lot of progress on discretizing the Hellinger-Reissner formulation.

This was the first motivation and application of BGG complexes in numerical analysis [6], see also [8, 33]. Recently, there has been a surge of interests on discretizing elasticity and other special cases of BGG complexes [3, 21, 20, 22, 19, 38, 39, 40, 47, 25, 27]. See also [42] for a review. Nevertheless, there seems to be no systematic discretization of either the BGG complexes or the entire BGG machinery behind them. The underlying machinery can have important consequences beyond the final complexes (see, e.g., [16] for connections between twisted de-Rham complexes and the Cosserat continua and [28] for deriving Poincaré operators using the BGG machinery). This gap is a major issue to address in order to use the BGG construction for numerical computation. We also mention that there are recent results on conforming simplicial finite elements for $(n-1)$-forms in $\mathbb{R}^n$ [23].

Restricted to the discrete level, the BGG machinery also provides a constructive tool for deriving discrete spaces by a diagram chasing. This idea has been developed at several places: a re-interpretation of the Arnold-Winther and Hu-Zhang elasticity elements [6, 26], conforming finite elements for linearized curvature on 2D triangular meshes [27], and a finite element elasticity complex on tetrahedral grids [25]. These results were derived in a case-by-case manner. In the context of isogeometric analysis (IGA) [30], spline de-Rham complexes can be found in, e.g., [15], and special cases of BGG complexes can be found in [3].

In this paper, we provide a systematic discretization of the BGG diagrams and complexes on cubical meshes. The resulting spaces are tensor products of spaces in one space dimension (1D). The tensor product construction is built upon two general assumptions on sequences in 1D. As examples of input spaces for 1D complexes, we consider both splines and finite elements. We verify that the assumptions of the construction in [10] on the continuous level hold for these tensor product spaces. The resulting discrete BGG diagram is symmetric in the sense that the space of (i, j)-forms is isomorphic to the space of (j, i)-forms as they have the same coefficients. The tensor product construction leads to bounded commuting (quasi-)interpolations for splines and finite elements, which are important for analyzing numerical schemes for PDEs. Thus, it provides us with a powerful tool to obtain stable discretizations on cubical meshes. It also avoids the issue of intrinsic super-smoothness (c.f. [36]) known from simplicial schemes.

The outline of the paper is as follows: In Section 1, we review the BGG construction at the continuous level, and in Section 2, we demonstrate how we construct tensor-product BGG complexes for arbitrary form degree and space dimension. In Sections 3 and 4, we derive spline and tensor product finite element BGG complexes and provide examples that include the elasticity complex, the div div complex and the Hessian complex. We note that our results are mostly based on [15, 14]. In Section 5, we provide a brief review of the main aspects of our construction and highlight our results. We also show why extending our construction to more delicate BGG complexes (e.g., the conformal complexes which require input of three de-Rham complexes [16]) is nontrivial.

1. BGG complexes of differential forms

1.1. **Review of the BGG construction.** We briefly review the main idea of the BGG construction. The BGG construction is a tool to derive more complexes from the de-Rham complexes. In the setup in [10], we consider the following *BGG diagram*:

$$
\begin{tikzcd}
0 \arrow[r] & Z^0 \arrow[r, "D^0"] & Z^1 \arrow[r, "D^1"] & \cdots \arrow[r, "D^{n-1}"] & Z^n \arrow[r] & 0 \\
0 \arrow[r] & \tilde{Z}^0 \arrow[r, "\tilde{D}^0"] \arrow[ur, "S^0"] & \tilde{Z}^1 \arrow[r, "\tilde{D}^1"] \arrow[ur, "S^1"] & \cdots \arrow[r, "\tilde{D}^{n-1}"] \arrow[ur, "S^{n-1}"] & \tilde{Z}^n \arrow[r] & 0.
\end{tikzcd}
\tag{1}
$$

Typically, each row of (1) is a scalar- or vector-valued de-Rham complex, and the two rows are connected by some algebraic operators $S^\bullet$ (in vector proxies, this can be, e.g., taking the skew-symmetric or the trace part of a matrix). We require that (1) is a commuting diagram, meaning that $D^{j+1}S^j = -S^{j+1}\tilde{D}^j$ for all $j = 0, \ldots, n-1$ (the sign is not important, but just for technical reasons). There is one index J such that S^J is bijective, and S^j are injective for $j \leq J$ and surjective for $j \geq J$. From a BGG diagram, we can read out a *BGG sequence*. The recipe is that we start from the first row, restricted to $\mathcal{R}(S)^\perp$ at each index (for example, if S is taking the skew-symmetric part of a matrix, then $\mathcal{R}(S)^\perp$ consists of symmetric matrices). Then at index J, we connect the two rows by constructing a new operator $\tilde{D}(S^J)^{-1}D$.

This is possible since S^J is bijective and corresponds to a zig-zag on the diagram. Then we come to the second row. For the rest of the indices $j > J$, we restrict the domains to $\mathcal{N}(S)$ in the second row. The final BGG complex is summarized as the following:

$$
\begin{aligned}
&0 \longrightarrow \Upsilon^0 \xrightarrow{\mathscr{D}^0} \Upsilon^1 \xrightarrow{\mathscr{D}^1} \cdots \xrightarrow{\mathscr{D}^{J-1}} \Upsilon^J \\
&\qquad \xrightarrow{\mathscr{D}^J} \Upsilon^{J+1} \xrightarrow{\mathscr{D}^{j+1}} \cdots \xrightarrow{\mathscr{D}^{n-1}} \Upsilon^n \longrightarrow 0,
\end{aligned}
\tag{2}
$$

with spaces

$$
\Upsilon^j := \begin{cases} Z^0, & j = 0, \\ \mathcal{R}(S^{j-1})^\perp, & 1 \leq j \leq J, \\ \mathcal{N}(S^j), & J < j \leq n, \end{cases}
\tag{3}
$$

and operators

$$
\mathscr{D}^j = \begin{cases} P_{\mathcal{R}(S^j)^\perp} D^j, & 0 \leq j < J, \\ \tilde{D}^j (S^j)^{-1} D^j, & j = J, \\ \tilde{D}^j, & J < j \leq n, \end{cases} \tag{4}
$$

where $P_{\mathcal{R}(S^j)^\perp}$ denotes the orthogonal projection onto $\mathcal{R}(S^j)^\perp$. The main conclusion of this construction is that, under some conditions, the cohomology of the BGG complex (2) is isomorphic to the cohomology of the input complexes in (1). For de-Rham complexes, the cohomology is known with a broad class of function spaces [29]. Various analytic properties follow from general arguments based on the fact that the cohomology being finite dimensional [10].

Example 1 (BGG complex in 1D). *The simplest example is in one space dimension. We consider the following diagram with any real number q*

$$
\begin{tikzcd}
0 \arrow[r] & H^q \arrow[r, "\partial_x"] & H^{q-1} \arrow[r] & 0 \\
0 \arrow[r] & H^{q-1} \arrow[r, "\partial_x"] \arrow[ur, "I"] & H^{q-2} \arrow[r] & 0.
\end{tikzcd} \tag{5}
$$

Here we only have one connecting operator, specifically, we have $S^0 = I$ identity operator, which is obviously bijective (one may also extend the diagram by adding zero maps). All the conditions for the BGG diagrams hold trivially. From (5) *we derive the BGG complex*

$$
0 \longrightarrow H^q \xrightarrow{\partial_x^2} H^{q-2} \longrightarrow 0. \tag{6}
$$

In this case, the BGG construction is just to connect the two first-order derivatives to get a second-order derivative. In this simple example it is also easy to verify our claim on the cohomology: the kernel of ∂_x (cohomology at index 0) in each row is $\mathbb{R}$. In the BGG complex (6)*, the kernel of ∂_x^2 (cohomology at index 0) is isomorphic to $\mathbb{R} \oplus \mathbb{R}$.*

1.2. **Application to alternating form-valued differential forms.** We follow the construction of alternating form-valued differential forms in [10]. For $i \geq 0$, let $\mathrm{Alt}^i \mathbb{R}^n$ be the space of algebraic i-forms, that is, of alternating i-linear maps on $\mathbb{R}^n$. We also set $\mathrm{Alt}^{i,j}\mathbb{R}^n = \mathrm{Alt}^i \mathbb{R}^n \otimes \mathrm{Alt}^j \mathbb{R}^n$, the space of $\mathrm{Alt}^j \mathbb{R}^n$-valued i-forms or, equivalently, the space of $(i+j)$-linear maps on $\mathbb{R}^n$ which are alternating in the first i variables and also in the last j variables. For the linking maps, we define the algebraic operators $s^{i,j} : \mathrm{Alt}^{i,j}\mathbb{R}^n \to$

$\mathrm{Alt}^{i+1,j-1}\mathbb{R}^n$

$$
\begin{aligned}
(7)\quad & s^{i,j}\mu(v_0,\cdots,v_i)(w_1,\cdots,w_{j-1}) \\
&\qquad := \sum_{l=0}^{i}(-1)^l \mu(v_0,\cdots,\widehat{v_l},\cdots,v_i)(v_l,w_1,\cdots,w_{j-1}), \\
&\qquad\qquad\qquad \forall v_0,\cdots,v_i,w_1,\cdots,w_{j-1}\in\mathbb{R}^n,
\end{aligned}
$$

where in each term of the alternating sum the *hat* denotes the suppressed vector, that is, the vector we move from the first parenthesis to the second (see the appendix in [10]). Alternatively, we have the following expression of $s^{i,j}$ on a basis of alternating forms: let $\sigma \in \Sigma(k,n)$ and $\tau \in \Sigma(m,n)$ be combinations of k and m elements of $\{1,\ldots,n\}$, respectively. Then,

$$
\begin{aligned}
(8)\quad & s^{k,m}(dx^{\sigma_1}\wedge\cdots\wedge dx^{\sigma_k}\otimes dx^{\tau_1}\wedge\cdots\wedge dx^{\tau_m}) \\
&= \sum_{l=1}^{m}(-1)^{l-1} dx^{\tau_l}\wedge dx^{\sigma_1}\wedge\cdots\wedge dx^{\sigma_k}\otimes dx^{\tau_1}\wedge\cdots\wedge\widehat{dx^{\tau_l}}\wedge\cdots\wedge dx^{\tau_m},
\end{aligned}
$$

where we move one factor from the second term in the tensor product to the first. For completeness, we include a detailed proof of equation (8) in Appendix B. From now on, we will omit $\mathbb{R}^n$ in the notation when confusion is unlikely. We also write $S^{i,j} = I\otimes s^{i,j} : H^q\otimes\mathrm{Alt}^{i,j} \to H^q\otimes\mathrm{Alt}^{i+1,j-1}$ for any Sobolev order q. We use $H^q\Lambda^i$ as another notation for $H^q\otimes\mathrm{Alt}^i$. We have the exterior derivative, $d^i : H^q\otimes\mathrm{Alt}^i \to H^{q-1}\otimes\mathrm{Alt}^{i+1}$. Tensorizing with Alt^j then gives $d^i : H^q\otimes\mathrm{Alt}^{i,j} \to H^{q-1}\otimes\mathrm{Alt}^{i+1,j}$. With these definitions, we may write down the diagram generalizing (5) to n dimensions:

(9)

$$
\begin{tikzcd}
0 \arrow[r] & H^q\otimes\mathrm{Alt}^{0,0} \arrow[r, "d"] & H^{q-1}\otimes\mathrm{Alt}^{1,0} \arrow[r, "d"] & \cdots \arrow[r, "d"] & H^{q-n}\otimes\mathrm{Alt}^{n,0} \arrow[r] & 0 \\
0 \arrow[r] & H^{q-1}\otimes\mathrm{Alt}^{0,1} \arrow[r, "d"] \arrow[ur, "S^{0,1}"] & H^{q-2}\otimes\mathrm{Alt}^{1,1} \arrow[r, "d"] \arrow[ur, "S^{1,1}"] & \cdots \arrow[r, "d"] \arrow[ur, "S^{n-1,1}"] & H^{q-n-1}\otimes\mathrm{Alt}^{n,1} \arrow[r] & 0 \\
 & \vdots & \vdots & & \vdots & \\
0 \arrow[r] & H^{q-n+1}\otimes\mathrm{Alt}^{0,n-1} \arrow[r, "d"] & H^{q-n}\otimes\mathrm{Alt}^{1,n-1} \arrow[r, "d"] & \cdots \arrow[r, "d"] & H^{q-2n+1}\otimes\mathrm{Alt}^{n,n-1} \arrow[r] & 0 \\
0 \arrow[r] & H^{q-n}\otimes\mathrm{Alt}^{0,n} \arrow[r, "d"] \arrow[ur, "S^{0,n}"] & H^{q-n-1}\otimes\mathrm{Alt}^{1,n} \arrow[r, "d"] \arrow[ur, "S^{1,n}"] & \cdots \arrow[r, "d"] \arrow[ur, "S^{n-1,n}"] & H^{q-2n}\otimes\mathrm{Alt}^{n,n} \arrow[r] & 0.
\end{tikzcd}
$$

Example 2 (BGG complexes in 3D)**.** *The BGG diagram* (9) *has the following vector/matrix proxies for $n = 3$, where the operators between proxies* *are defined in Appendix A:*

(10)

$$\begin{tikzcd}
0 \arrow[r] & H^q \otimes \mathbb{R} \arrow[r, "\mathrm{grad}"] & H^{q-1} \otimes \mathbb{V} \arrow[r, "\mathrm{curl}"] & H^{q-2} \otimes \mathbb{V} \arrow[r, "\mathrm{div}"] & H^{q-3} \otimes \mathbb{R} \arrow[r] & 0 \\
0 \arrow[r] & H^{q-1} \otimes \mathbb{V} \arrow[r, "\mathrm{grad}"] \arrow[ur, "I"] & H^{q-2} \otimes \mathbb{M} \arrow[r, "\mathrm{curl}"] \arrow[ur, "2\,\mathrm{vskw}"] & H^{q-3} \otimes \mathbb{M} \arrow[r, "\mathrm{div}"] \arrow[ur, "\mathrm{tr}"] & H^{q-4} \otimes \mathbb{V} \arrow[r] & 0 \\
0 \arrow[r] & H^{q-2} \otimes \mathbb{V} \arrow[r, "\mathrm{grad}"] \arrow[ur, "-\mathrm{mskw}"] & H^{q-3} \otimes \mathbb{M} \arrow[r, "\mathrm{curl}"] \arrow[ur, "\mathcal{T}"] & H^{q-4} \otimes \mathbb{M} \arrow[r, "\mathrm{div}"] \arrow[ur, "2\,\mathrm{vskw}"] & H^{q-5} \otimes \mathbb{V} \arrow[r] & 0 \\
0 \arrow[r] & H^{q-3} \otimes \mathbb{R} \arrow[r, "\mathrm{grad}"] \arrow[ur, "\iota"] & H^{q-4} \otimes \mathbb{V} \arrow[r, "\mathrm{curl}"] \arrow[ur, "-\mathrm{mskw}"] & H^{q-5} \otimes \mathbb{V} \arrow[r, "\mathrm{div}"] \arrow[ur, "I"] & H^{q-6} \otimes \mathbb{R} \arrow[r] & 0.
\end{tikzcd}$$

Here $\mathbb{V} := \mathbb{R}^n$ *denotes vectors and* $\mathbb{M}$ *is the space of all* $n \times n$*-matrices. Let further* $\mathbb{S}$, $\mathbb{K}$, *and* $\mathbb{T}$ *be the subspaces of matrices that are symmetric, skew-symmetric and trace-free, respectively. Following the BGG recipe, from the first two rows of* (10) *we obtain the Hessian complex*

(11)

$$0 \longrightarrow H^q \otimes \mathbb{R} \xrightarrow{\mathrm{hess}} H^{q-2} \otimes \mathbb{S} \xrightarrow{\mathrm{curl}} H^{q-3} \otimes \mathbb{T} \xrightarrow{\mathrm{div}} H^{q-4} \otimes \mathbb{V} \longrightarrow 0,$$

where $\mathrm{hess} := \mathrm{grad}\,\mathrm{grad}$. *From the second and third rows of* (10) *we obtain the elasticity complex*

(12)

$$0 \longrightarrow H^{q-1} \otimes \mathbb{V} \xrightarrow{\mathrm{def}} H^{q-2} \otimes \mathbb{S} \xrightarrow{\mathrm{inc}} H^{q-4} \otimes \mathbb{S} \xrightarrow{\mathrm{div}} H^{q-5} \otimes \mathbb{V} \longrightarrow 0.$$

Here $\mathrm{def} := \mathrm{sym}\,\mathrm{grad}$ *is the linearized deformation (symmetric part of gradient) and* $\mathrm{inc} = \mathrm{curl}\,\mathcal{T}^{-1}\,\mathrm{curl}$ *leads to the linearized Einstein tensor. Finally, the last two rows of* (10) *yield the divdiv complex*

(13)

$$0 \to H^{q-2} \otimes \mathbb{V} \xrightarrow{\mathrm{dev}\,\mathrm{grad}} H^{q-3} \otimes \mathbb{T} \xrightarrow{\mathrm{sym}\,\mathrm{curl}} H^{q-4} \otimes \mathbb{S} \xrightarrow{\mathrm{div}\,\mathrm{div}} H^{q-6} \otimes \mathbb{V} \to 0.$$

Remark 1. *In the construction of simplicial finite elements or splines, the isomorphism between the* grad-rot *version of complexes and the* curl-div *version is obtained by swapping the tangent and normal directions. In the tensor product construction, this is obtained via changing parametric directions accordingly.*

Example 3 (BGG Complex in 2D)**.** *Let* $\mathrm{sskw} = \mathrm{mskw}^{-1} \circ \mathrm{skw} : \mathbb{M} \to \mathbb{R}$ *be the map taking the skew part of a matrix and identifying it with a scalar (see* [10]*).*

A 2D version of the diagram (10) *is*

$$
\begin{tikzcd}
0 \arrow[r] & H^q \otimes \mathbb{R} \arrow[r, "\mathrm{grad}"] & H^{q-1} \otimes \mathbb{V} \arrow[r, "\mathrm{rot}"] & H^{q-2} \otimes \mathbb{R} \arrow[r] & 0 \\
0 \arrow[r] & H^{q-1} \otimes \mathbb{V} \arrow[r, "\mathrm{grad}"] \arrow[ur, "I"] & H^{q-2} \otimes \mathbb{M} \arrow[r, "\mathrm{rot}"] \arrow[ur, "-2\,\mathrm{sskw}"] & H^{q-3} \otimes \mathbb{V} \arrow[r] & 0 \\
0 \arrow[r] & H^{q-2} \otimes \mathbb{R} \arrow[r, "\mathrm{grad}"] \arrow[ur, "\mathrm{mskw}"] & H^{q-3} \otimes \mathbb{V} \arrow[r, "\mathrm{rot}"] \arrow[ur, "I"] & H^{q-4} \otimes \mathbb{R} \arrow[r] & 0.
\end{tikzcd}
\tag{14}
$$

Although the injectivity/surjectivity conditions are not necessary for running the BGG machinery [16], we will stick to these conditions in our construction on the discrete level, for simplicity. To summarize, on the discrete level, we seek discrete versions of the BGG diagrams such that the injectivity/surjectivity conditions are preserved. Then the commutativity $DS = -S\tilde{D}$ is trivially following the results on the continuous level. To this end, we need discrete de-Rham complexes for the two rows in the construction, respectively. In fact, this is rather easy to see in 1D. To discretize (5), we want to construct discrete spaces $V_h^{i,j}$ that fit in the following diagram

$$
\begin{tikzcd}
0 \arrow[r] & V_h^{0,0} \arrow[r, "\partial_x"] & V_h^{1,0} \arrow[r] & 0 \\
0 \arrow[r] & V_h^{0,1} \arrow[r, "\partial_x"] \arrow[ur, "I"] & V_h^{1,1} \arrow[r] & 0.
\end{tikzcd}
\tag{15}
$$

The connecting map (the identity map) makes sense if $V_h^{1,0} \cong V_h^{0,1}$. This means that the first row has higher regularity than the second. This is a general pattern in the BGG construction, but becomes more complicated in higher dimensions.

2. Tensor product construction

In this section, we present a general construction. The idea is that we start with a diagram in 1D, and extend it to $\mathbb{R}^n$ by tensor product. This process is mostly algebraic and does not depend on a particular construction in 1D. Thus, we start with a fairly abstract assumption.

2.1. A discrete BGG complex in 1D.

The general construction is based on the following assumption.

Assumption 1. *Let $\mathcal{I} := [0,1]$, and $L^2\Lambda^i(\mathcal{I}) := L^2(\mathcal{I}) \otimes \mathrm{Alt}^i\mathbb{R}$. For an abstract smoothness parameter $\mathbf{r}$ and integer $p \geq 1$, let $\mathcal{S}_{\mathbf{r}}^p$ be a finite dimensional subspace of $L^2(\mathcal{I})$ and thus $\mathcal{S}_{\mathbf{r}}^p\Lambda^i(\mathcal{I}) := \mathcal{S}_{\mathbf{r}}^p \otimes \mathrm{Alt}^i\mathbb{R}$ be a finite dimensional subspace of $L^2\Lambda^i(\mathcal{I})$. Furthermore, we assume that the sequence*

$$
0 \longrightarrow \mathcal{S}_{\mathbf{r}}^p\Lambda^0(\mathcal{I}) \xrightarrow{d^0} \mathcal{S}_{\mathbf{r}-1}^{p-1}\Lambda^1(\mathcal{I}) \longrightarrow 0 \tag{16}
$$

is a complex and d^0 is onto.

As we shall see later in specific examples, $\mathcal{S}^p_{\mathbf{r}}(\mathcal{I})$ may be a spline space on $\mathcal{I}$ of degree p with regularity vector $\mathbf{r}$ (see Section 3) or a finite element space of degree p and interelement continuity r (see Section 4). The decreasing indices in (16) reflect the fact that d^0 is a first-order differential operator. For splines, since $\mathbf{r}$ is a vector, $\mathbf{r} \geq 0$ means every component of $\mathbf{r}$ is non-negative. Similarly, in expressions such as $\mathbf{r} - a$ where $a \in \mathbb{R}$, a is subtracted from each component, see for instance [15, p.821].

When there is no danger of confusion, we omit $\mathcal{I}$ in the notation. Now we tensor the spaces in (16) with alternating forms and obtain with the above notation

$$\mathscr{S}^p_{\mathbf{r}}\Lambda^{i,j}(\mathcal{I}) := \mathcal{S}^{p-i-j}_{\mathbf{r}-i-j}\Lambda^{i,j}(\mathcal{I}) := \mathcal{S}^{p-i-j}_{\mathbf{r}-i-j} \otimes \mathrm{Alt}^i\mathbb{R} \otimes \mathrm{Alt}^j\mathbb{R}, \tag{17}$$

as the space of 1D alternating i,j-forms with coefficients in $\mathcal{S}^{p-i-j}_{\mathbf{r}-i-j}$. Following Assumption 1, the following sequences are complexes for $j = 0, 1$ and d^0 is onto:

$$0 \longrightarrow \mathcal{S}^{p-j}_{\mathbf{r}-j}\Lambda^{0,j}(\mathcal{I}) \xrightarrow{d^0} \mathcal{S}^{p-1-j}_{\mathbf{r}-1-j}\Lambda^{1,j}(\mathcal{I}) \longrightarrow 0. \tag{18}$$

Hence, we obtain a 1D BGG diagram that satisfies the assumptions in Section 1:

$$\begin{tikzcd}
0 \arrow[r] & \mathcal{S}^p_{\mathbf{r}}\Lambda^{0,0}(\mathcal{I}) \arrow[r, "d^0"] & \mathcal{S}^{p-1}_{\mathbf{r}-1}\Lambda^{1,0}(\mathcal{I}) \arrow[r] & 0 \\
0 \arrow[r] & \mathcal{S}^{p-1}_{\mathbf{r}-1}\Lambda^{0,1}(\mathcal{I}) \arrow[r, "d^0"] \arrow[ur, "S^{0,1}"] & \mathcal{S}^{p-2}_{\mathbf{r}-2}\Lambda^{1,1}(\mathcal{I}) \arrow[r] & 0.
\end{tikzcd} \tag{19}$$

Remark 2. *In a vector proxy with canonical bases, $S^{0,1}$ boils down to the identity operator. In one dimension, there is only one $s^{k,m}$ operator according to (7), namely $s^{0,1}\colon \mathrm{Alt}^{0,1} \to \mathrm{Alt}^{1,0}$. Nevertheless, it will be useful for the construction of tensor products, namely Lemma 1, to define $s^{k,m} \equiv 0$ for all other $k, m \in \{0, 1\}$.*

2.2. **Tensor product spaces and the exterior derivative.** Let

$$\sigma = (\sigma_1, \dots, \sigma_k) \in \Sigma(k, n)$$

be a combination of k numbers from $\{1, \cdots, n\}$ such that $1 \leq \sigma_1 < \cdots < \sigma_k \leq n$. Define the set of characteristic vectors

$$X_k := \left\{ \boldsymbol{\chi} = (\chi_1, \cdots, \chi_n) \in \{0,1\}^n \,\middle|\, \sum_{j=1}^{n} \chi_j = k \right\}. \tag{20}$$

Then, the characteristic vector of a combination $\sigma \in \Sigma(k, n)$ is the vector $\boldsymbol{\chi}(\sigma) \in X_k$, such that

$$\chi_i(\sigma) = \begin{cases} 1, & i \in \sigma, \\ 0, & i \notin \sigma. \end{cases}$$

Using combinations, we can define a basis for $\mathrm{Alt}^k\mathbb{R}^n$ consisting of elements

$$\begin{aligned} dx^\sigma &= dx^{\sigma_1} \wedge \cdots \wedge dx^{\sigma_k} && \sigma \in \Sigma(k,n), \\ &= (dx^1)^{s_1} \wedge \cdots \wedge (dx^n)^{s_n} && \boldsymbol{s} = \boldsymbol{\chi}(\sigma) \in X_k. \end{aligned}$$

Here, we define $(dx^i)^1 = dx^i$ and $(dx^i)^0 = 1$. Note that these are two different notations for the same form and we will use both of them below for convenience. For $\boldsymbol{\chi} \in X_n$ we introduce the notation

$$|\boldsymbol{\chi}|_m := \sum_{l=1}^{m} \chi_l, \tag{21}$$

with the convention $|\boldsymbol{\chi}|_0 = 0$.

In $\mathbb{R}^n$, define the unit hypercube $\mathcal{I}^n := [0,1]^n$. We define the following Sobolev spaces of alternating forms:

$$\begin{aligned} L^2\Lambda^{i,j}(\mathcal{I}^n) &:= L^2\Lambda^i(\mathcal{I}^n) \otimes \mathrm{Alt}^j\mathbb{R}^n = L^2(\mathcal{I}^n) \otimes \mathrm{Alt}^{i,j}\mathbb{R}^n, \\ H^q\Lambda^{i,j}(\mathcal{I}^n) &:= H^q\Lambda^i(\mathcal{I}^n) \otimes \mathrm{Alt}^j\mathbb{R}^n = H^q(\mathcal{I}^n) \otimes \mathrm{Alt}^{i,j}\mathbb{R}^n. \end{aligned}$$

Let $\sigma \in \Sigma(i,n)$ and $\tau \in \Sigma(j,n)$ be combinations with characteristic vectors $\boldsymbol{s} = \boldsymbol{\chi}(\sigma)$ and $\boldsymbol{t} = \boldsymbol{\chi}(\tau)$, respectively. Let $\omega_k = \alpha_k (dx)^{s_k} \otimes (dx)^{t_k} \in L^2\Lambda^{s_k,t_k}$ for $k = 1, \ldots, n$ be one-dimensional differential forms with an L^2 coefficient α_k. Then, the n-dimensional tensor product is defined as

$$\begin{aligned} &\omega_1 \otimes \cdots \otimes \omega_n \\ &\quad = (\alpha_1 \otimes \cdots \otimes \alpha_n)(dx^1)^{s_1} \wedge \cdots \wedge (dx^n)^{s_n} \otimes (dx^1)^{t_1} \wedge \cdots \wedge (dx^n)^{t_n} \\ &\quad = (\alpha_1 \otimes \cdots \otimes \alpha_n) dx^\sigma \otimes dx^\tau \\ &\quad = (\alpha_1 \otimes \cdots \otimes \alpha_n)[(dx^1)^{s_1} \otimes (dx^1)^{t_1}] \wedge \cdots \wedge [(dx^n)^{s_n} \otimes (dx^n)^{t_n}]. \end{aligned}$$

Here we have used different combinations of wedge and tensor products to express the same object. The different notations are used in various contexts below and should be clear from these identities. We define the tensor product spaces:

$$\begin{aligned} L^2\Lambda^{k,l}_{\otimes n}(\mathcal{I}^n) &:= \bigoplus_{\substack{(i_i,\cdots,i_n)\in X_k \\ (j_1,\cdots,j_n)\in X_l}} L^2\Lambda^{i_1,j_1}(\mathcal{I}) \otimes L^2\Lambda^{i_2,j_2}(\mathcal{I}) \otimes \cdots \otimes L^2\Lambda^{i_n,j_n}(\mathcal{I}) \\ &= \bigoplus_{\substack{(i_i,\cdots,i_n)\in X_k \\ (j_1,\cdots,j_n)\in X_l}} L^2(\mathcal{I}^n) \otimes \mathrm{Alt}^{i_1,j_1} \otimes \cdots \otimes \mathrm{Alt}^{i_n,j_n}, \end{aligned} \tag{22}$$

$$
\begin{aligned}
\mathscr{S}^{\vec{p}}_{\vec{\mathbf{r}}}\Lambda^{k,l} &:= \bigoplus_{\substack{(i_i,\cdots,i_n)\in X_k\\(j_1,\cdots,j_n)\in X_l}} \mathscr{S}^{p_1}_{\mathbf{r}_1}\Lambda^{i_1,j_1}(\mathcal{I})\otimes\cdots\otimes\mathscr{S}^{p_n}_{\mathbf{r}_n}\Lambda^{i_n,j_n}(\mathcal{I})\\
&= \bigoplus_{\substack{(i_i,\cdots,i_n)\in X_k\\(j_1,\cdots,j_n)\in X_l}} \mathcal{S}^{p_1-i_1-j_1}_{\mathbf{r}_1-i_1-j_1}\Lambda^{i_1,j_1}(\mathcal{I})\otimes\cdots\otimes\mathcal{S}^{p_n-i_n-j_n}_{\mathbf{r}_n-i_n-j_n}\Lambda^{i_n,j_n}(\mathcal{I})\\
&= \bigoplus_{\substack{(i_i,\cdots,i_n)\in X_k\\(j_1,\cdots,j_n)\in X_l}} \left(\mathcal{S}^{p_1-i_1-j_1}_{\mathbf{r}_1-i_1-j_1}\otimes\cdots\otimes\mathcal{S}^{p_n-i_n-j_n}_{\mathbf{r}_n-i_n-j_n}\right)\otimes\mathrm{Alt}^{i_1,j_1}\otimes\cdots\otimes\mathrm{Alt}^{i_n,j_n}.
\end{aligned}\tag{23}
$$

Note that, the spaces $L^2\Lambda^{k,l}(\mathcal{I}^n)$ and $L^2\Lambda^{k,l}_{\otimes n}(\mathcal{I}^n)$ coincide, see [37, Example 3.7]. Equations (22) and (23) give a characterization that separates the coefficients and the alternating form basis.

We discuss the definition of the discrete spaces $\mathscr{S}^{\vec{p}}_{\vec{\mathbf{r}}}\Lambda^{k,l}$. First, the sums over $i_1+\cdots+i_n=k$ and $j_1+\cdots+j_n=l$ follow the general definition of tensor products of alternating forms. Second, for each individual space $\mathcal{S}^{p_t-i_t-j_t}_{\mathbf{r}_t-i_t-j_t}\Lambda^{i_t,j_t}(\mathcal{I})$, the pattern is that higher form indices correspond to lower "polynomial degrees" and "regularity" (although at this stage we have not introduced splines or finite elements, so these terms are only understood formally). This is readily understood for the first indices, as derivatives lower degree and regularity by one. Then we observe that the s operators are an alternating sum which moves one factor dx^j from the right to the left (see Lemma 6). In this operation, the sum of i_t and j_t remains unchanged for any $1\le t\le n$ (this fact will be formalized in Lemma 1 below). This means in order that the discrete spaces are compatible with the S operators, i.e., S maps the discrete space $\mathscr{S}^{\vec{p}}_{\vec{\mathbf{r}}}\Lambda^{k,l}$ to the right one $\mathscr{S}^{\vec{p}}_{\vec{\mathbf{r}}}\Lambda^{k+1,l-1}$, the definition should always involve the sum i_h+j_h. This explains the pattern in $\mathcal{S}^{p_t-i_t-j_t}_{\mathbf{r}_t-i_t-j_t}$. This further leads to a pattern in the discretization of the BGG diagram (9), i.e., the (k,l)-th space is isomorphic to the (l,k)-th space, as the polynomial coefficients in the definition of $\mathscr{S}^{\vec{p}}_{\vec{\mathbf{r}}}\Lambda^{k,l}$ are invariant when we switch k and l. For example, the first row of (9) is a standard tensor product de-Rham complex [5, 24], and *so is the first column.* As a more specific example, the 3D elasticity complex starts with a (0, 1)-form (the first space in the second row of (10)), indicating that our discrete elasticity complex starts from a Nédélec space. See Section 4 for more details.

The exterior derivatives $d^k:\mathcal{S}^p_{\mathbf{r}}\Lambda^{k,l}(\mathcal{I})\to\mathcal{S}^{p-1}_{\mathbf{r}-1}\Lambda^{k+1,l}(\mathcal{I})$ follow from the standard definition. These operators extend naturally to $\mathscr{S}^{\vec{p}}_{\vec{\mathbf{r}}}\Lambda^{k,l}$ with Cartesian and tensor products (see [5]), yielding $d^k\colon\mathscr{S}^{\vec{p}}_{\vec{\mathbf{r}}}\Lambda^{k,l}\to\mathscr{S}^{\vec{p}}_{\vec{\mathbf{r}}}\Lambda^{k+1,l}$ given by

$$
d^k(u_1\otimes\cdots\otimes u_n)=\sum_{s=1}^{n}(-1)^{|\boldsymbol{i}|_{s-1}}(u_1\otimes\cdots\otimes du_s\otimes\cdots\otimes u_n),
$$

for all $u_l\in\mathcal{S}^{p_l-i_l-j_l}_{\mathbf{r}_l-i_l-j_l}\Lambda^{i_l,j_l}(\mathcal{I})$, with $\boldsymbol{i}\in X_k$, and $\boldsymbol{j}\in X_l$.

2.3. **Tensor product BGG complexes.** To derive the BGG complexes, we first establish a BGG diagram with the spaces obtained above by means of the tensor product construction,

(24)
$$\begin{tikzcd}
\cdots \arrow[r] & \mathscr{S}_{\vec{\mathbf{r}}}^{\vec{p}}\Lambda^{i-1,J-1} \arrow[r, "d"] & \mathscr{S}_{\vec{\mathbf{r}}}^{\vec{p}}\Lambda^{i,J-1} \arrow[r, "d"] & \mathscr{S}_{\vec{\mathbf{r}}}^{\vec{p}}\Lambda^{i+1,J-1} \arrow[r] & \cdots \\
\cdots \arrow[r] \arrow[ur] & \mathscr{S}_{\vec{\mathbf{r}}}^{\vec{p}}\Lambda^{i-1,J} \arrow[r, "d"] \arrow[ur, "S^{i-1,J}"] & \mathscr{S}_{\vec{\mathbf{r}}}^{\vec{p}}\Lambda^{i,J} \arrow[r, "d"] \arrow[ur, "S^{i,J}"] & \mathscr{S}_{\vec{\mathbf{r}}}^{\vec{p}}\Lambda^{i+1,J} \arrow[r] \arrow[ur] & \cdots .
\end{tikzcd}$$

Now, we verify that it satisfies the conditions in Section 1, i.e., commutativity $DS = -S\tilde{D}$ and the injectivity/surjectivity conditions. Since $\mathscr{S}_{\vec{\mathbf{r}}}^{\vec{p}}\Lambda^{\bullet}$ are subspaces of $L^2\Lambda^{\bullet}$, the commutativity follows from the continuous level. We will further verify that $S^{k,l} = I \otimes s^{k,l}$ maps between the discrete spaces in the diagram. We start deriving an explicit expression of the operator $s^{k,l}$ on tensor product alternating forms.

Lemma 1. *Let $\boldsymbol{i} \in X_k$, $\boldsymbol{j} \in X_l$ and $\omega_h \in \mathrm{Alt}^{i_h,j_h}\mathbb{R}$ for $h = 1, \cdots, n$. Then, $\omega = \omega_1 \otimes \cdots \otimes \omega_n \in \mathrm{Alt}^k\mathbb{R}^n \otimes \mathrm{Alt}^l\mathbb{R}^n$ and there holds*
$$s^{k,l}\omega = \sum_{h=1}^{n} (-1)^{|\boldsymbol{i}|_h + |\boldsymbol{j}|_h} \omega_1 \wedge \cdots \wedge s^{i_h,j_h}\omega_h \wedge \cdots \wedge \omega_n$$

Proof. We prove this lemma for basis forms and conclude the general statement by linearity. Hence, let $\omega_h = (dx^h)^{i_h} \otimes (dx^h)^{j_h}$. Note that, as observed in Remark 2, there holds
$$s^{i_h,j_h}\omega_h = \begin{cases} dx^h \otimes 1 & \text{if } i_h = 0, j_h = 1 \\ 0 & \text{else.} \end{cases} \tag{25}$$

Using (8), and recalling (21), we find:
$$\begin{aligned}
s^{k,l}\omega &= s^{k,l}\big(((dx^1)^{i_1} \wedge \cdots \wedge (dx^n)^{i_n}) \otimes ((dx^1)^{j_1} \wedge \cdots \wedge (dx^n)^{j_n})\big) \\
&= \sum_{h=1}^{n} (-1)^{|\boldsymbol{i}|_h + 1} \delta_{1,j_h} \big((dx^h)^{j_h} \wedge (dx^1)^{i_1} \wedge \cdots \wedge (dx^n)^{i_n}\big) \\
&\qquad \otimes \big((dx^1)^{j_1} \wedge \cdots \wedge \widehat{(dx^h)^{j_h}} \wedge \cdots \wedge (dx^n)^{j_n}\big) \\
&= \sum_{h=1}^{n} (-1)^{|\boldsymbol{i}|_h + 1} \delta_{1,j_h} \big((dx^h)^{j_h} \otimes 1\big) \wedge \omega_1 \wedge \cdots \wedge \big((dx^h)^{i_h} \otimes 1\big) \wedge \cdots \wedge \omega_n \\
&= \sum_{h=1}^{n} (-1)^{|\boldsymbol{i}|_h + |\boldsymbol{j}|_h} \delta_{1,j_h} \omega_1 \wedge \cdots \wedge \big((dx^h)^{j_h} \otimes 1\big) \wedge \big((dx^h)^{i_h} \otimes 1\big) \wedge \cdots \wedge \omega_n.
\end{aligned}$$

Note that
$$\begin{aligned}
\delta_{1,j_h}\big((dx^h)^{j_h} \otimes 1\big) \wedge \big((dx^h)^{i_h} \otimes 1\big) &= \delta_{1,j_h}\big((dx^h)^{j_h} \wedge (dx^h)^{i_h}\big) \otimes 1 \\
&= s^{i_h,j_h}\big((dx^h)^{i_h} \otimes (dx^h)^{j_h}\big) = s^{i_h,j_h}\omega_h.
\end{aligned}$$

In particular, for $j_h = 1$, we can assume $i_h = 0$, since otherwise we would have a two-form on $\mathbb{R}$, which must be zero. Hence, the lemma is proven. $\square$

Remark 3. *Let $u = q \otimes \omega \in \mathscr{S}_{\vec{\mathbf{r}}}^{\vec{p}}\Lambda^{k,l}$. Since $S^{k,l} = I \otimes s^{k,l}$ as in the continuous case, $S^{k,l}u = q \otimes s^{k,l}\omega$. By the definition in* (23)*, the polynomial spaces on the left and on the right of $S^{k,l}$ are the same since adding to i subtracts from j. This implies that the induced mapping between the coefficient spaces is bijective. Hence, $S^{k,l}\mathscr{S}_{\vec{\mathbf{r}}}^{\vec{p}}\Lambda^{k,l} \subset \mathscr{S}_{\vec{\mathbf{r}}}^{\vec{p}}\Lambda^{k+1,l-1}$ and $S^{k,l}$ inherits surjectivity from $s^{k,l}$.*

Following the BGG recipe in Section 1, and exploiting the bijectivity of $S^{J-1,J}$, we obtain the discrete spaces

$$\Upsilon_h^i := \begin{cases} \mathcal{R}(S^{i-1,J})^\perp \subset \mathscr{S}_{\vec{\mathbf{r}}}^{\vec{p}}\Lambda^{i,J-1}, & i < J; \\ \mathcal{N}(S^{i,J}) \subset \mathscr{S}_{\vec{\mathbf{r}}}^{\vec{p}}\Lambda^{i,J}, & i \geq J, \end{cases}$$

and the operators

$$\mathscr{D}^i := \begin{cases} P_{\mathcal{R}(S^{i-1,J})^\perp} d^i, & i \leq J-1; \\ d^i \circ (S^{i-1,J})^{-1} \circ d^i, & i = J; \\ d^i, & i \geq J+1, \end{cases}$$

where h is used as a generic index for discrete spaces. The derived discrete BGG complex is

$$0 \longrightarrow \Upsilon_h^0 \xrightarrow{\mathscr{D}^0} \Upsilon_h^1 \xrightarrow{\mathscr{D}^1} \cdots \xrightarrow{\mathscr{D}^{n-1}} \Upsilon_h^n \longrightarrow 0. \tag{26}$$

Thus, we have the algebraic setup in Section 1 with the discrete spaces $\mathscr{S}_{\vec{\mathbf{r}}}^{\vec{p}}\Lambda^{k,l}$. Following [10, Theorem 6], the main conclusion is the cohomology of the derived BGG complex.

Theorem 1. *The dimension of cohomology of* (26) *is bounded by that of the input complexes, i.e.,*

$$\dim \mathscr{H}^k(\Upsilon_h^\bullet, \mathscr{D}^\bullet) \leq \dim \mathscr{H}^k(\mathscr{S}_{\vec{\mathbf{r}}}^{\vec{p}}\Lambda^{\bullet,J-1}, d^\bullet) + \dim \mathscr{H}^k(\mathscr{S}_{\vec{\mathbf{r}}}^{\vec{p}}\Lambda^{\bullet,J}, d^\bullet). \tag{27}$$

Remark 4. *The construction in* [10] *has two levels. First, by the commutativity and the injectivity/surjectivity condition of $S^\bullet$, we can conclude with an inequality of dimension as Theorem 1. Second, if more structures are available (referred to as the K operators in* [10] *satisfying $S = dK - Kd$), then the inequality becomes an equality. All the examples in this paper satisfy this further condition on the continuous level. Nevertheless, whether* (27) *is an equality (thus reflecting the correct cohomology) or not is not clear at this stage as the K operators may not map between the right discrete spaces.*

2.4. **Quasi-interpolation operators.** Interpolation operators are an important theoretical tool for verifying the convergence of numerical schemes in finite element methods and isogeometric analysis. In this section, we obtain interpolation operators for the tensor product BGG complexes (26) from versions in 1D. The key assumption is that we have these operators for both rows in a 1D BGG diagram in (19), and the operators satisfy certain conditions when we connect the two rows ((29) below). This will be highlighted in Assumption 2 below. Again, the discussions in this section are abstract in the sense that no splines or finite elements are involved. The main conclusion is that we can input bounded commuting maps from continuous spaces to discrete spaces in 1D, and derive the corresponding BGG version in nD by using only the algebraic structures of tensor products.

The discussions will be based on the following assumption.

Assumption 2. *There exists $\pi^{i,j} : L^2\Lambda^{i,j}(\mathcal{I}) \to \mathscr{S}_{\mathbf{r}}^{p}\Lambda^{i,j}(\mathcal{I})$, where $i,j = 0,1$ in 1D, that is L^2-bounded*

$$\|\pi^{i,j}u\| \leq C\|u\|,$$

satisfying the commutativity condition

$$d^i\pi^{i,j} = \pi^{i+1,j}d^i. \tag{28}$$

Moreover, we require that

$$S^{i,j}\pi^{i,j} = \pi^{i+1,j-1}S^{i,j}. \tag{29}$$

Note that the only nontrivial case for (29) is $i = 0$ and $j = 1$.

In vector proxy, $S^{0,1}$ is just identity and $\mathcal{S}_{\mathbf{r}-1}^{p-1}\Lambda^{0,1}$ is identical to $\mathcal{S}_{\mathbf{r}-1}^{p-1}\Lambda^{1,0}$. The commutativity of (29) would follow from the arguments in Section 2.2 once we use equivalent quasi-interpolation operators for the two spaces in the 1D BGG diagram connected by the S^0 operator. Thus, to satisfy Assumption 2, we need to have a consistent set of three bounded commuting quasi-interpolation operators.

Remark 5. *For later convenience, we extend the quasi-interpolation operator $\pi^{i,j}$ by 0, whenever applied to differential forms with index not equal to (i,j). For example, for $i = 0$ and $j = 1$, $\pi^{0,1}$ is defined on $L^2\Lambda^{0,1}(\mathcal{I})$ according to Assumption 2, and it is extended to 0, whenever applied to $L^2\Lambda^{0,0}(\mathcal{I})$, $L^2\Lambda^{1,0}(\mathcal{I})$ or $L^2\Lambda^{1,1}(\mathcal{I})$.*

Making use of Remark 5 and following [14], we give the following definition.

Definition 1. *Given the quasi-interpolation operators in 1D, we define the tensor product quasi-interpolation operator in n dimensions for $k,l = 0,\ldots,n$*

$$\pi_{\otimes n}^{k,l} \colon L^2\Lambda_{\otimes n}^{k,l} \to \mathscr{S}_{\vec{\mathbf{r}}}^{\vec{p}}\Lambda^{k,l}$$

as follows:

$$\pi_{\otimes n}^{k,l} \coloneqq \sum_{\substack{(i_i,\cdots,i_n)\in X_k\\(j_1,\cdots,j_n)\in X_l}} \pi^{i_1,j_1}\otimes\cdots\otimes\pi^{i_n,j_n}. \tag{30}$$

Let us detail the particular case, where $\pi^{k,l}_{\otimes n}$ is applied to rank one tensor product differential forms. Let $\omega = \omega_1 \otimes \cdots \otimes \omega_n \in L^2\Lambda^{k,l}_{\otimes n}$, with $\omega_t \in L^2\Lambda^{i_t,j_t}(\mathcal{I})$, $\boldsymbol{i} = (i_1, \cdots, i_n) \in X_k$, $\boldsymbol{j} = (j_1, \cdots, j_n) \in X_l$. Then, we get

$$\begin{aligned}\pi^{k,l}_{\otimes n}\omega &:= (\pi^{i_1,j_1} \otimes \cdots \otimes \pi^{i_n,j_n})(\omega_1 \otimes \cdots \otimes \omega_n)\\ &= \pi^{i_1,j_1}\omega_1 \otimes \cdots \otimes \pi^{i_n,j_n}\omega_n.\end{aligned}$$

Next, we will show that the tensor product operators defined in (30) are bounded and commute with the differential operators $\mathscr{D}^\bullet$ in the BGG complexes (26). Note that the operators $\mathscr{D}^\bullet$ are a composition of $d^\bullet$, $P_{\mathcal{R}}(S)^\perp$ and S^{-1}, depending on the indices (4). To prove that $\pi^\bullet_\otimes$ commutes with $\mathscr{D}^\bullet$, we will show that $\pi^\bullet_\otimes$ commutes with each one of these operators. This will be established in Lemmas 2 to 4 below.

Lemma 2. *$\pi^\bullet_{\otimes n}$ commutes with $d^\bullet$, i.e.,*

$$d^k\pi^{k,l}_{\otimes n} = \pi^{k+1,l}_{\otimes n}d^k. \tag{31}$$

Proof. It is sufficient to show the result on rank one tensor product differential forms. By linearity and density, the conclusion holds for all elements in $L^2\Lambda^{k,l}_{\otimes n}$. For any $\omega_t \in L^2\Lambda^{i_t,j_t}(\mathcal{I})$, $\boldsymbol{i} = (i_1, \cdots, i_n) \in X_k$, $\boldsymbol{j} = (j_1, \cdots, j_n) \in X_l$, (see [14, (31)])

$$d^k(\omega_1 \otimes \omega_2 \otimes \cdots \otimes \omega_n) = \sum_{t=1}^{n}(-1)^{|\boldsymbol{i}|_{t-1}}(\omega_1 \otimes \cdots \otimes d^{i_l}\omega_l \otimes \cdots \otimes \omega_n).$$

Then the conclusion follows from the commutativity (28) in 1D. □

Lemma 3. *$\pi^\bullet_{\otimes n}$ commutes with $S^\bullet$, i.e.,*

$$\pi^{k+1,l-1}_{\otimes n}S^{k,l} = S^{k,l}\pi^{k,l}_{\otimes n}, \quad \forall\ 0 \le k \le n-1,\ 1 \le l \le n. \tag{32}$$

Proof. The conclusion follows from Lemma 1 and the commutativity (29) in Assumption 2. □

By Assumption 2, in 1D, we have $\pi^{i,j} : L^2\Lambda^{i,j}(\mathcal{I}) \to \mathcal{S}^p_{\mathbf{r}}\Lambda^{i,j}(\mathcal{I}),\ i,j = 0,1$. Let $\{dx^\sigma \otimes dx^\mu\}_{\sigma\in\Sigma(i,n),\mu\in\Sigma(j,n)}$ be a basis of $\mathrm{Alt}^{i,j}$. Then $\pi^{i,j}$ induces a unique map $\tilde{\pi}^{i,j} : L^2(\mathcal{I}) \to \mathcal{S}^p_{\mathbf{r}}$ between the coefficients, satisfying

$$\pi^{i,j} = \tilde{\pi}^{i,j} \otimes I. \tag{33}$$

Lemma 4. *The following commutativity property holds:*

$$\pi^{k,l}_{\otimes n}(I \otimes P_{\mathcal{R}(s^{k-1,l+1})^\perp}) = (I \otimes P_{\mathcal{R}(s^{k-1,l+1})^\perp})\pi^{k,l}_{\otimes n}. \tag{34}$$

Proof. The claim follows by observing that $\pi^{k,l}_{\otimes n}$ acts on the coefficient function, whereas it is the identity operator on alternating forms; on the contrary,

$I \otimes P_{\mathcal{R}(s^{k-1,l+1})^\perp}$ acts only on alternating forms as shown in the following:

$$\begin{aligned}
\pi_{\otimes n}^{k,l}\left(I \otimes P_{\mathcal{R}(s^{k-1,l+1})^\perp}\right) &= \left(\tilde{\pi}_{\otimes n}^{k,l} \otimes I\right)\left(I \otimes P_{\mathcal{R}(s^{k-1,l+1})^\perp}\right) \\
&= \tilde{\pi}_{\otimes n}^{k,l} \otimes P_{\mathcal{R}(s^{k-1,l+1})^\perp} = \left(I \otimes P_{\mathcal{R}(s^{k-1,l+1})^\perp}\right)\left(\tilde{\pi}_{\otimes n}^{k,l} \otimes I\right) \\
&= \left(I \otimes P_{\mathcal{R}(s^{k-1,l+1})^\perp}\right)\pi_{\otimes n}^{k,l}.
\end{aligned}$$

□

From (31), (32), (34) and the explicit form of the operators in the BGG complexes (4), we obtain the main result.

Theorem 2. *The $\pi_{\otimes n}$ operators commute with $\mathscr{D}$ defined in* (4)*, i.e.,*

$$\pi_{\otimes n}^{k+1,l-1}\mathscr{D}^k = \mathscr{D}^k \pi_{\otimes n}^{k,l}.$$

Define

$$\mathbb{E}^k = \begin{cases} \mathcal{R}(s^{k-1,l+1})^\perp, & k \le l, \\ \mathcal{N}(s^{k,l+1}), & k \ge l+1, \end{cases}$$

and the spaces

$$H(\mathscr{D}^k) := \{u \in L^2 \otimes \mathbb{E}^k : \mathscr{D}^k u \in L^2 \otimes \mathbb{E}^{k+1}\} \tag{35}$$

with the graph norm $\|u\|^2_{H(\mathscr{D}^k)} := \|u\|^2 + \|\mathscr{D}^k u\|^2$.

Theorem 3. *The operators $\pi_{\otimes n}^{k,l}$ are bounded in L^2- and $H(\mathscr{D}^k)$-norms, i.e., there exist positive constants C such that*

$$\|\pi_{\otimes n}^{k,l} u\| \le C\|u\|, \qquad \forall u \in L^2 \otimes \mathbb{E}^k, \tag{36}$$

$$\|\pi_{\otimes n}^{k,l} u\|_{H(\mathscr{D}^k)} \le C\|u\|_{H(\mathscr{D}^k)}, \qquad \forall u \in H(\mathscr{D}^k). \tag{37}$$

Proof. The L^2-boundedness of $\pi_{\otimes n}^{k,l}$ is similar to [14, Lemma 7]. In particular, there holds:

$$\|\pi_{\otimes n}^{k,l}\|_* \le \sum_{\substack{\boldsymbol{i}\in X_k \\ \boldsymbol{j}\in X_l}} \|\pi^{i_1,j_1} \otimes \cdots \otimes \pi^{i_n,j_n}\|_* = \sum_{\substack{\boldsymbol{i}\in X_k \\ \boldsymbol{j}\in X_l}} \|\pi^{i_1,j_1}\|_* \cdots \|\pi^{i_n,j_n}\|_*,$$

where $\|\cdot\|_*$ denotes the L^2-norm of operators. Canonical argument, see [35, Theorem 8.4], shows that the L^2-boundedness and commutativity implies boundedness in the $H(\mathscr{D}^k)$-norm. □

3. Spline BGG complexes

In this section, we derive spline BGG complexes that satisfy Assumption 1 and Assumption 2 for arbitrary space dimensions and present the elasticity, Hessian and div div complexes as examples. The outline of the section is as follows: In Section 3.1, we state some basic concepts from the spline theory and define a spline BGG complex in 1D along with quasi-interpolation operators for the 1D spline spaces. In Section 3.2, we discretize the diagram

(14) and the 2D version of the diagram (10) using spline spaces and present the derivation of the 2D stress complex as a BGG complex. In Section 3.3, we discretize the diagram (10) for vector proxies in higher dimensions using spline spaces and present the derivation of the elasticity, Hessian, and div div complexes as BGG complexes.

3.1. **Splines in 1D.** Splines are piecewise polynomial functions that satisfy certain regularity conditions. By convention, their parametric domain is defined as the unit interval $\mathcal{I} = [0, 1]$ in 1D. Knot vectors are used to partition $\mathcal{I}$ and define the spline basis functions. A knot vector is a vector Σ given by $\Sigma = [\eta_1, \ldots, \eta_{n+p+1}]$ where its components, a.k.a., the knot values (or the knots), satisfy $0 \leq \eta_1 \leq \eta_2 \leq \cdots \leq \eta_{n+p+1} \leq 1$, n denotes the dimension of the spline space and p denotes the polynomial degree of the spline. The regularity of a spline defined via Σ is given by a vector $\mathbf{r}$ that consists of the regularity values of the spline at the knot values in Σ.

Suppose Σ includes N distinct knot values and let $\hat{\Sigma} \subseteq \Sigma$ be the set of these distinct knot values. For example, if $\Sigma = \{0.0, 0.0, 0.2, 0.4, 1.0, 1.0\}$, then $\hat{\Sigma} := \{0.0, 0.2, 0.4, 1.0\}$. The regularity of a spline at a knot value $\hat{\eta}_i \in \hat{\Sigma}$ is computed by $r_i := p - m_i$ where $1 \leq m_i \leq p + 1$ denotes the number of times the knot value $\hat{\eta}_i$ is repeated in Σ. By utilizing the definition in [48], we may define the one-dimensional spline space $S^p_{\mathbf{r}}(\Sigma)$ as follows:

$$
\begin{aligned}
S^p_{\mathbf{r}}(\Sigma) := \{\phi : \exists \phi_i \in \mathcal{P}_p : \phi(x) = \phi_i(x) \text{ for } x \in I_i := [\hat{\eta}_{i-1}, \hat{\eta}_i),\ \hat{\eta}_i \in \hat{\Sigma}, I_i \subset \mathcal{I},\\
i = 1, \ldots (N-1), D^{r_i}\phi_{i-1}(\hat{\eta}_i) = D^{r_i}\phi_i(\hat{\eta}_i),\ r_i = 0, 1, \ldots, p - m_i\},
\end{aligned}
$$

where $\mathcal{P}_p$ denotes the polynomial space of degree p.

Remark 6. *Note that if $m_i = m$ for some $m \geq 1$ and $\forall \hat{\eta}_i \in \Sigma$, then $S^p_{\mathbf{r}}(\Sigma)$ becomes a regular polynomial space of degree p defined piecewise over the knot intervals in I.*

In this paper, we consider splines given by open knot vectors, that is, the case where $\eta_1 = \cdots = \eta_{p+1}$ and $\eta_{n+1} = \cdots = \eta_{n+p+1}$, and use B-splines (a.k.a. basis splines) since every spline function can be written as a linear combination of B-splines of the same degree [46]. Thus, we refer to B-splines by the term *spline* here.
B-spline basis functions of degree p denoted by $\{B^p_i\}$ are defined via the Cox-de Boor formula [32], which starts with defining the lowest degree basis functions $\{B^0_i(\eta)\}$ and obtains the higher degree B-spline basis functions $\{B^p_i(\eta)\}$ by recursion as follows:

$$
B^0_i(\eta) := \begin{cases} 1, & \eta_i \leq \eta < \eta_{i+1}, \\ 0, & \text{otherwise}, \end{cases}
$$

$$
B^p_i(\eta) = \frac{\eta - \eta_i}{\eta_{i+p} - \eta_i} B^{p-1}_i(\eta) + \frac{\eta_{i+p+1} - \eta}{\eta_{i+p+1} - \eta_{i+1}} B^{p-1}_{i+1}(\eta).
$$

Using these basis functions, we may also define $S^p_{\mathbf{r}}(\Sigma)$ as follows:

$$
S^p_{\mathbf{r}}(\Sigma) := \operatorname{span}\{B^p_i(\eta) : i = 1, \ldots, n\}. \tag{38}
$$

Suppose that $r_i \geq 0$ at the internal knots, that is, the B-spline functions are at least continuous at the knots, then the derivative of a B-spline basis function is given by

$$\frac{d}{d\eta}B_i^p(\eta) = \frac{p}{\eta_{i+p} - \eta_i}B_i^{p-1}(\eta) - \frac{p}{\eta_{i+p+1} - \eta_{i+1}}B_{i+1}^{p-1}(\eta),$$

where $B_1^{p-1}(\eta) = B_{n+1}^{p-1}(\eta) = 0$, by assumption [31]. We note that $d : S_{\mathbf{r}}^p(\Sigma) \to S_{\mathbf{r}-1}^{p-1}(\tilde{\Sigma})$ is surjective where $\tilde{\Sigma} = \{\eta_2, \eta_3, \ldots, \eta_{n+p}\}$ is an open knot vector obtained by dropping the first and the last knots from the open knot vector Σ [31].

In the rest of the text, to maintain a compatible notation with the finite element spaces used in the BGG construction in Section 4.1, we use $S_{\mathbf{r}}^p(\mathcal{I})$ to denote a B-spline space of degree p with regularity $\mathbf{r}$ defined over $\mathcal{I}$, excluding the knot vector Σ from the notation. Thus, we denote the space of i-forms with coefficients in $S_{\mathbf{r}}^p(\mathcal{I})$ by $S_{\mathbf{r}}^p\Lambda^i(\mathcal{I})$ as in Section 2.

By the definition of $S_{\mathbf{r}}^p\Lambda^i(\mathcal{I})$, it follows that the following sequence is a complex and d is onto for any integer-valued vector $\mathbf{r}$ defined as above and any scalar $p \geq 2$. Thus, Assumption 1 is satisfied.

$$0 \longrightarrow \mathcal{S}_{\mathbf{r}}^p\Lambda^0(\mathcal{I}) \xrightarrow{d} \mathcal{S}_{\mathbf{r}-1}^{p-1}\Lambda^1(\mathcal{I}) \longrightarrow 0.$$

Now, we need to verify Assumption 2. We first define the following quasi-interpolation operator as the one defined in [31]:

$$\tilde{\pi}_0^p : L^2(\mathcal{I}) \to S_{\mathbf{r}}^p(\mathcal{I}), \qquad \tilde{\pi}_0^p(u) := \sum_{i=1}^{n} \lambda_i^p(u)B_i^p, \tag{39}$$

where each λ_i^p is the dual basis functional to the B-spline basis function B_i^p(See Theorem 4.41 in [48]). Thus, we have $\lambda_i^p(B_j^p) = \delta_{ij}$ for $i, j = 1, 2, \cdots, n$. As pointed out in [31], this dual basis is used for it enables the satisfaction of the L^2-stability of the interpolation operators. Then, we may uniquely define $\tilde{\pi}_1^{p-1} : L^2(\mathcal{I}) \to S_{\mathbf{r}-1}^{p-1}(\mathcal{I})$ using (39)

$$\tilde{\pi}_1^{p-1}v := \frac{d}{d_x}\tilde{\pi}_0^p \int_0^x v(s)\ ds.$$

Similarly, we define $\tilde{\pi}_2^{p-2} : L^2(\mathcal{I}) \to S_{\mathbf{r}-2}^{p-2}(\mathcal{I})$

$$\tilde{\pi}_2^{p-2}v := \frac{d}{d_x}\tilde{\pi}_1^{p-1} \int_0^x v(s)\ ds.$$

Note that $\tilde{\pi}_0^p$ and $\tilde{\pi}_1^{p-1}$ are spline preserving, therefore, projections. $\tilde{\pi}_0^p$ is L^2-stable, and $\tilde{\pi}_1^{p-1}$ is L^2-stable when the mesh is quasi-uniform [31]. Similarly, $\tilde{\pi}_2^{p-2}$ is spline preserving and L^2-stable when the mesh is quasi-uniform. Moreover, these projection operators commute with the differential operators, that is for $i = 0, 1$, we have

$$\tilde{\pi}_{i+1}^{p-(i+1)} \partial_x v = \partial_x \tilde{\pi}_i^{p-i} v. \tag{40}$$

Then, we use these projection operators to define the quasi-interpolation operators $\pi^{i,j} : L^2\Lambda^{i,j}(\mathcal{I}) \to \mathcal{S}_{\mathbf{r}-i-j}^{p-i-j}\Lambda^{i,j}(\mathcal{I})$ as in Section 2.4. For example, $\pi^{0,0} : L^2\Lambda^{0,0}(\mathcal{I}) \to \mathcal{S}_{\mathbf{r}}^{p}\Lambda^{0,0}(\mathcal{I})$ is given by $\pi^{0,0}w = (\tilde{\pi}^{0,0}u)(1 \otimes 1) = (\tilde{\pi}_0^p u)(1 \otimes 1)$ where $w = u(1 \otimes 1) \in L^2\Lambda^{0,0}$. Then, let $w = u(dx^{\sigma_1} \otimes 1) \in L^2\Lambda^{1,0}(\mathcal{I})$ and define $\pi^{1,0} : L^2\Lambda^{1,0}(\mathcal{I}) \to S_{\mathbf{r}-1}^{p-1}\Lambda^{1,0}(\mathcal{I})$, as follows:

$$\pi^{1,0}w = \pi^{1,0}u(dx^{\sigma_1} \otimes 1) = (\tilde{\pi}^{1,0}u)(dx^{\sigma_1} \otimes 1) = (\tilde{\pi}_1^{p-1}u)(dx^{\sigma_1} \otimes 1).$$

We define $\pi^{0,1} = \pi^{1,0}$ taking advantage of the equivalence of the relevant spline spaces. Similarly, we define $\pi^{1,1} : L^2\Lambda^{1,1}(\mathcal{I}) \to S_{\mathbf{r}-2}^{p-2}\Lambda^{1,1}(\mathcal{I})$ as follows:

$$\begin{aligned}\pi^{1,1}w = \pi^{1,1}u(dx^{\sigma_1} \otimes dx^{\mu_1}) &= (\tilde{\pi}^{1,1}u)(dx^{\sigma_1} \otimes dx^{\mu_1}) \\ &= (\tilde{\pi}_2^{p-2}u)(dx^{\sigma_1} \otimes dx^{\mu_1}),\end{aligned}$$

where $w = u(dx^{\sigma_1} \otimes dx^{\mu_1}) \in L^2\Lambda^{1,1}(\mathcal{I})$. We see that (28) holds due to (40). Moreover, (29) holds due to the definition of the spaces and interpolation operators, that is, $S^{0,1}\pi^{0,1} = \pi^{1,0}S^{0,1}$. Thus, the assumptions in Section 1 are satisfied, and we can write the 1D BGG diagram as follows:

$$\begin{tikzcd} 0 \arrow[r] & \mathcal{S}_{\mathbf{r}}^{p}(\mathcal{I}) \arrow[r, "d"] & \mathcal{S}_{\mathbf{r}-1}^{p-1}(\mathcal{I}) \arrow[r] & 0 \\ 0 \arrow[r] & \mathcal{S}_{\mathbf{r}-1}^{p-1}(\mathcal{I}) \arrow[r, "d"] \arrow[ur, "I"] & \mathcal{S}_{\mathbf{r}-2}^{p-2}(\mathcal{I}) \arrow[r] & 0. \end{tikzcd} \tag{41}$$

From (41), we derive the BGG complex

$$0 \longrightarrow \mathcal{S}_{\mathbf{r}}^{p}(\mathcal{I}) \xrightarrow{d \circ I \circ d} \mathcal{S}_{\mathbf{r}-2}^{p-2}(\mathcal{I}) \longrightarrow 0.$$

3.2. **Splines in higher dimensions.** In $\mathbb{R}^n$, we define the spline spaces over the tensor-product of parametric domain as $\mathcal{I} = [0,1]^n$. The partition of $\mathcal{I}$ is determined by n knot vectors such that an element (with non-zero measure) on the parametric domain is $I_{\boldsymbol{i}} = [\eta_{i_1}^1, \eta_{i_1+1}^1] \otimes \cdots \otimes [\eta_{i_n}^n, \eta_{i_n+1}^n]$ where $\eta_{i_j} \neq \eta_{i_j+1}$. Let $\mathbf{r}_i$ denote the fiber of $\vec{\mathbf{r}}$ in direction i, thus being the regularity vector in this coordinate direction. Then, a spline space in n dimensions is defined via the tensor product of one-dimensional spline spaces, that is, $\mathcal{S}_{\vec{\mathbf{r}}}^{\vec{p}} = \mathcal{S}_{\mathbf{r}_1}^{p_1} \otimes \mathcal{S}_{\mathbf{r}_2}^{p_2} \otimes \cdots \otimes \mathcal{S}_{\mathbf{r}_n}^{p_n}$ where $S_{\mathbf{r}_i}^{p_i}$ denotes the spline defined over the i^{th} coordinate direction.

For simplicity, we focus on the case $n = 2$. We discretize the 2D version of the second and third rows in the diagram (10) via two-dimensional spline

spaces as follows:
(42)

$$\begin{tikzcd}
0 \arrow[r] & \mathcal{S}^{p_1,p_2}_{\mathbf{r}_1,\mathbf{r}_2} \arrow[r, "\mathrm{curl}"] & \begin{pmatrix} \mathcal{S}^{p_1,p_2-1}_{\mathbf{r}_1,\mathbf{r}_2-1} \\ \mathcal{S}^{p_1-1,p_2}_{\mathbf{r}_1-1,\mathbf{r}_2} \end{pmatrix} \arrow[r, "\mathrm{div}"] & \mathcal{S}^{p_1-1,p_2-1}_{\mathbf{r}_1-1,\mathbf{r}_2-1} \arrow[r] & 0 \\
0 \arrow[r] & \begin{pmatrix} \mathcal{S}^{p_1,p_2-1}_{\mathbf{r}_1,\mathbf{r}_2-1} \\ \mathcal{S}^{p_1-1,p_2}_{\mathbf{r}_1-1,\mathbf{r}_2} \end{pmatrix} \arrow[r, "\mathrm{curl}"] \arrow[ur, "I"] & \begin{pmatrix} \mathcal{S}^{p_1,p_2-2}_{\mathbf{r}_1,\mathbf{r}_2-2} & \mathcal{S}^{p_1-1,p_2-1}_{\mathbf{r}_1-1,\mathbf{r}_2-1} \\ \mathcal{S}^{p_1-1,p_2-1}_{\mathbf{r}_1-1,\mathbf{r}_2-1} & \mathcal{S}^{p_1-2,p_2}_{\mathbf{r}_1-2,\mathbf{r}_2} \end{pmatrix} \arrow[r, "\mathrm{div}"] \arrow[ur, "2\,\mathrm{vskw}"] & \begin{pmatrix} \mathcal{S}^{p_1-1,p_2-2}_{\mathbf{r}_1-1,\mathbf{r}_2-2} \\ \mathcal{S}^{p_1-2,p_2-1}_{\mathbf{r}_1-2,\mathbf{r}_2-1} \end{pmatrix} \arrow[r] & 0.
\end{tikzcd}$$

Note that the spaces in the first row of (42) are chosen so as to yield a vector-valued de-Rham complex, and we start the second row using the connecting map $S = I$ and complete it in a similar fashion. Since this diagram fulfills the necessary conditions for the BGG construction, we can derive the 2D (stress) elasticity complex as a BGG complex:

$$0 \longrightarrow \mathcal{S}^{p_1,p_2}_{\mathbf{r}_1,\mathbf{r}_2} \xrightarrow{\mathrm{curl}\,\mathrm{curl}} \Sigma_h \xrightarrow{\mathrm{div}} \begin{pmatrix} \mathcal{S}^{p_1-1,p_2-2}_{\mathbf{r}_1-1,\mathbf{r}_2-2} \\ \mathcal{S}^{p_1-2,p_2-1}_{\mathbf{r}_1-2,\mathbf{r}_2-1} \end{pmatrix} \longrightarrow 0, \tag{43}$$

where

$$\Sigma_h := \left\{ \sigma_h = \begin{pmatrix} \sigma_{11} & \sigma_{12} \\ \sigma_{21} & \sigma_{22} \end{pmatrix} \in \begin{pmatrix} \mathcal{S}^{p_1,p_2-2}_{\mathbf{r}_1,\mathbf{r}_2-2} & \mathcal{S}^{p_1-1,p_2-1}_{\mathbf{r}_1-1,\mathbf{r}_2-1} \\ \mathcal{S}^{p_1-1,p_2-1}_{\mathbf{r}_1-1,\mathbf{r}_2-1} & \mathcal{S}^{p_1-2,p_2}_{\mathbf{r}_1-2,\mathbf{r}_2} \end{pmatrix} : \sigma_{12} = \sigma_{21} \right\},$$

and $\mathrm{curl}\,\mathrm{curl}\, v = \begin{bmatrix} \frac{\partial^2 v}{\partial x_2^2} & -\frac{\partial^2 v}{\partial x_1 \partial x_2} \\ -\frac{\partial^2 v}{\partial x_1 \partial x_2} & \frac{\partial^2 v}{\partial x_1^2} \end{bmatrix}$ for $v \in \mathcal{S}^{p_1,p_2}_{\mathbf{r}_1,\mathbf{r}_2}$.

In the light of Remark 1, we also consider the following discretization of the first two rows of the diagram (14) via two-dimensional spline spaces.
(44)

$$\begin{tikzcd}
0 \arrow[r] & \mathcal{S}^{p_1,p_2}_{\mathbf{r}_1,\mathbf{r}_2} \arrow[r, "\mathrm{grad}"] & \begin{pmatrix} \mathcal{S}^{p_1-1,p_2}_{\mathbf{r}_1-1,\mathbf{r}_2} \\ \mathcal{S}^{p_1,p_2-1}_{\mathbf{r}_1,\mathbf{r}_2-1} \end{pmatrix} \arrow[r, "\mathrm{rot}"] & \mathcal{S}^{p_1-1,p_2-1}_{\mathbf{r}_1-1,\mathbf{r}_2-1} \arrow[r] & 0 \\
0 \arrow[r] & \begin{pmatrix} \mathcal{S}^{p_1-1,p_2}_{\mathbf{r}_1-1,\mathbf{r}_2} \\ \mathcal{S}^{p_1,p_2-1}_{\mathbf{r}_1,\mathbf{r}_2-1} \end{pmatrix} \arrow[r, "\mathrm{grad}"] \arrow[ur, "\mathrm{I}"] & \begin{pmatrix} \mathcal{S}^{p_1-2,p_2}_{\mathbf{r}_1-2,\mathbf{r}_2} & \mathcal{S}^{p_1-1,p_2-1}_{\mathbf{r}_1-1,\mathbf{r}_2-1} \\ \mathcal{S}^{p_1-1,p_2-1}_{\mathbf{r}_1-1,\mathbf{r}_2-1} & \mathcal{S}^{p_1,p_2-2}_{\mathbf{r}_1,\mathbf{r}_2-2} \end{pmatrix} \arrow[r, "\mathrm{rot}"] \arrow[ur, "-2\,\mathrm{sskw}"] & \begin{pmatrix} \mathcal{S}^{p_1-2,p_2-1}_{\mathbf{r}_1-2,\mathbf{r}_2-1} \\ \mathcal{S}^{p_1-1,p_2-2}_{\mathbf{r}_1-1,\mathbf{r}_2-2} \end{pmatrix} \arrow[r] & 0.
\end{tikzcd}$$

We note that the diagram (44) yields the 2D rotated (stress) elasticity complex:

$$0 \longrightarrow \mathcal{S}^{p_1,p_2}_{\mathbf{r}_1,\mathbf{r}_2} \xrightarrow{\mathrm{hess}} \Sigma_h \xrightarrow{\mathrm{rot}} \begin{pmatrix} \mathcal{S}^{p_1-2,p_2-1}_{\mathbf{r}_1-2,\mathbf{r}_2-1} \\ \mathcal{S}^{p_1-1,p_2-2}_{\mathbf{r}_1-1,\mathbf{r}_2-2} \end{pmatrix} \longrightarrow 0, \tag{45}$$

where $\hat{\Sigma}_h$ is defined by

$$\hat{\Sigma}_h := \left\{ \sigma_h = \begin{pmatrix} \sigma_{11} & \sigma_{12} \\ \sigma_{21} & \sigma_{22} \end{pmatrix} \in \begin{pmatrix} \mathcal{S}^{p_1-2,p_2}_{\mathbf{r}_1-2,\mathbf{r}_2} & \mathcal{S}^{p_1-1,p_2-1}_{\mathbf{r}_1-1,\mathbf{r}_2-1} \\ \mathcal{S}^{p_1-1,p_2-1}_{\mathbf{r}_1-1,\mathbf{r}_2-1} & \mathcal{S}^{p_1,p_2-2}_{\mathbf{r}_1,\mathbf{r}_2-2} \end{pmatrix} : \sigma_{12} = \sigma_{21} \right\},$$

3.3. **Vector proxies for splines in three dimensions.** In this subsection, we discretize the diagram (10) via spline spaces in three-dimensions as follows:

$$
\begin{tikzcd}
0 \arrow[r] & V^{0,0} \arrow[r, "\mathrm{grad}"] & V^{1,0} \arrow[r, "\mathrm{curl}"] & V^{2,0} \arrow[r, "\mathrm{div}"] & V^{3,0} \arrow[r] & 0 \\
0 \arrow[r] & V^{0,1} \arrow[r, "\mathrm{grad}"] \arrow[ur, "\mathrm{I}"] & V^{1,1} \arrow[r, "\mathrm{curl}"] \arrow[ur, "2\,\mathrm{vskw}"] & V^{2,1} \arrow[r, "\mathrm{div}"] \arrow[ur, "\mathrm{tr}"] & V^{3,1} \arrow[r] & 0 \\
0 \arrow[r] & V^{0,2} \arrow[r, "\mathrm{grad}"] \arrow[ur, "-\mathrm{mskw}"] & V^{1,2} \arrow[r, "\mathrm{curl}"] \arrow[ur, "\mathcal{T}"] & V^{2,2} \arrow[r, "\mathrm{div}"] \arrow[ur, "2\,\mathrm{vskw}"] & V^{3,2} \arrow[r] & 0 \\
0 \arrow[r] & V^{0,3} \arrow[r, "\mathrm{grad}"] \arrow[ur, "\iota"] & V^{1,3} \arrow[r, "\mathrm{curl}"] \arrow[ur, "-\,\mathrm{mskw}"] & V^{2,3} \arrow[r, "\mathrm{div}"] \arrow[ur, "I"] & V^{3,3} \arrow[r] & 0,
\end{tikzcd}
\tag{46}
$$

where $\iota : \mathbb{R} \to \mathbb{M}$ is defined by $\iota u := uI$, and $\mathcal{T} : \mathbb{M} \to \mathbb{M}$ is defined as $\mathcal{T}u := u^t - tr(u)I$ [10]. We start with defining $V^{0,0} := \mathcal{S}^{p_1,p_2,p_3}_{\mathbf{r}_1,\mathbf{r}_2,\mathbf{r}_3}$. The rest of the first row is defined via following the sequence as follows:

(47)
$$
V^{1,0} = \begin{pmatrix} \mathcal{S}^{p_1-1,p_2,p_3}_{\mathbf{r}_1-1,\mathbf{r}_2,\mathbf{r}_3} \\ \mathcal{S}^{p_1,p_2-1,p_3}_{\mathbf{r}_1,\mathbf{r}_2-1,\mathbf{r}_3} \\ \mathcal{S}^{p_1,p_2,p_3-1}_{\mathbf{r}_1,\mathbf{r}_2,\mathbf{r}_3-1} \end{pmatrix}, \quad V^{2,0} = \begin{pmatrix} \mathcal{S}^{p_1,p_2-1,p_3-1}_{\mathbf{r}_1,\mathbf{r}_2-1,\mathbf{r}_3-1} \\ \mathcal{S}^{p_1-1,p_2,p_3-1}_{\mathbf{r}_1-1,\mathbf{r}_2,\mathbf{r}_3-1} \\ \mathcal{S}^{p_1-1,p_2-1,p_3}_{\mathbf{r}_1-1,\mathbf{r}_2-1,\mathbf{r}_3} \end{pmatrix}, \quad V^{3,0} = \mathcal{S}^{p_1-1,p_2-1,p_3-1}_{\mathbf{r}_1-1,\mathbf{r}_2-1,\mathbf{r}_3-1}.
$$

In the second row, we employ the symmetry of the diagram to obtain $V^{0,1} = V^{1,0}$. Then, via differential operations, we derive

$$
V^{1,1} = \begin{pmatrix} \mathcal{S}^{p_1-2,p_2,p_3}_{\mathbf{r}_1-2,\mathbf{r}_2,\mathbf{r}_3} & \mathcal{S}^{p_1-1,p_2-1,p_3}_{\mathbf{r}_1-1,\mathbf{r}_2-1,\mathbf{r}_3} & \mathcal{S}^{p_1-1,p_2,p_3-1}_{\mathbf{r}_1-1,\mathbf{r}_2,\mathbf{r}_3-1} \\ \mathcal{S}^{p_1-1,p_2-1,p_3}_{\mathbf{r}_1-1,\mathbf{r}_2-1,\mathbf{r}_3} & \mathcal{S}^{p_1,p_2-2,p_3}_{\mathbf{r}_1,\mathbf{r}_2-2,\mathbf{r}_3} & \mathcal{S}^{p_1,p_2-1,p_3-1}_{\mathbf{r}_1,\mathbf{r}_2-1,\mathbf{r}_3-1} \\ \mathcal{S}^{p_1-1,p_2,p_3-1}_{\mathbf{r}_1-1,\mathbf{r}_2,\mathbf{r}_3-1} & \mathcal{S}^{p_1,p_2-1,p_3-1}_{\mathbf{r}_1,\mathbf{r}_2-1,\mathbf{r}_3-1} & \mathcal{S}^{p_1,p_2,p_3-2}_{\mathbf{r}_1,\mathbf{r}_2,\mathbf{r}_3-2} \end{pmatrix}, \tag{48}
$$

$$
V^{2,1} = \begin{pmatrix} \mathcal{S}^{p_1-1,p_2-1,p_3-1}_{\mathbf{r}_1-1,\mathbf{r}_2-1,\mathbf{r}_3-1} & \mathcal{S}^{p_1-2,p_2,p_3-1}_{\mathbf{r}_1-2,\mathbf{r}_2,\mathbf{r}_3-1} & \mathcal{S}^{p_1-2,p_2-1,p_3}_{\mathbf{r}_1-2,\mathbf{r}_2-1,\mathbf{r}_3} \\ \mathcal{S}^{p_1,p_2-2,p_3-1}_{\mathbf{r}_1,\mathbf{r}_2-2,\mathbf{r}_3-1} & \mathcal{S}^{p_1-1,p_2-1,p_3-1}_{\mathbf{r}_1-1,\mathbf{r}_2-1,\mathbf{r}_3-1} & \mathcal{S}^{p_1-1,p_2-2,p_3}_{\mathbf{r}_1-1,\mathbf{r}_2-2,\mathbf{r}_3} \\ \mathcal{S}^{p_1,p_2-1,p_3-2}_{\mathbf{r}_1,\mathbf{r}_2-1,\mathbf{r}_3-2} & \mathcal{S}^{p_1-1,p_2,p_3-2}_{\mathbf{r}_1-1,\mathbf{r}_2,\mathbf{r}_3-2} & \mathcal{S}^{p_1-1,p_2-1,p_3-1}_{\mathbf{r}_1-1,\mathbf{r}_2-1,\mathbf{r}_3-1} \end{pmatrix}, \tag{49}
$$

$$
V^{3,1} = \begin{pmatrix} \mathcal{S}^{p_1-2,p_2-1,p_3-1}_{\mathbf{r}_1-2,\mathbf{r}_2-1,\mathbf{r}_3-1} \\ \mathcal{S}^{p_1-1,p_2-2,p_3-1}_{\mathbf{r}_1-1,\mathbf{r}_2-2,\mathbf{r}_3-1} \\ \mathcal{S}^{p_1-1,p_2-1,p_3-2}_{\mathbf{r}_1-1,\mathbf{r}_2-1,\mathbf{r}_3-2} \end{pmatrix}.
$$

In the third row, again by the symmetry of the diagram we have $V^{0,2} = V^{2,0}$, and by transposing $V^{2,1}$ we obtain

$$
V^{1,2} = \begin{pmatrix} \mathcal{S}^{p_1-1,p_2-1,p_3-1}_{\mathbf{r}_1-1,\mathbf{r}_2-1,\mathbf{r}_3-1} & \mathcal{S}^{p_1,p_2-2,p_3-1}_{\mathbf{r}_1,\mathbf{r}_2-2,\mathbf{r}_3-1} & \mathcal{S}^{p_1,p_2-1,p_3-2}_{\mathbf{r}_1,\mathbf{r}_2-1,\mathbf{r}_3-2} \\ \mathcal{S}^{p_1-2,p_2,p_3-1}_{\mathbf{r}_1-2,\mathbf{r}_2,\mathbf{r}_3-1} & \mathcal{S}^{p_1-1,p_2-1,p_3-1}_{\mathbf{r}_1-1,\mathbf{r}_2-1,\mathbf{r}_3-1} & \mathcal{S}^{p_1-1,p_2,p_3-2}_{\mathbf{r}_1-1,\mathbf{r}_2,\mathbf{r}_3-2} \\ \mathcal{S}^{p_1-2,p_2-1,p_3}_{\mathbf{r}_1-2,\mathbf{r}_2-1,\mathbf{r}_3} & \mathcal{S}^{p_1-1,p_2-2,p_3}_{\mathbf{r}_1-1,\mathbf{r}_2-2,\mathbf{r}_3} & \mathcal{S}^{p_1-1,p_2-1,p_3-1}_{\mathbf{r}_1-1,\mathbf{r}_2-1,\mathbf{r}_3-1} \end{pmatrix}.
$$

The remaining spaces are defined by similar arguments as follows:

$$V^{2,2} = \begin{pmatrix} \mathcal{S}^{p_1,p_2-2,p_3-2}_{\mathbf{r}_1,\mathbf{r}_2-2,\mathbf{r}_3-2} & \mathcal{S}^{p_1-1,p_2-1,p_3-2}_{\mathbf{r}_1-1,\mathbf{r}_2-1,\mathbf{r}_3-2} & \mathcal{S}^{p_1-1,p_2-2,p_3-1}_{\mathbf{r}_1-1,\mathbf{r}_2-2,\mathbf{r}_3-1} \\ \mathcal{S}^{p_1-1,p_2-1,p_3-2}_{\mathbf{r}_1-1,\mathbf{r}_2-1,\mathbf{r}_3-2} & \mathcal{S}^{p_1-2,p_2,p_3-2}_{\mathbf{r}_1-2,\mathbf{r}_2,\mathbf{r}_3-2} & \mathcal{S}^{p_1-2,p_2-1,p_3-1}_{\mathbf{r}_1-2,\mathbf{r}_2-1,\mathbf{r}_3-1} \\ \mathcal{S}^{p_1-1,p_2-2,p_3-1}_{\mathbf{r}_1-1,\mathbf{r}_2-2,\mathbf{r}_3-1} & \mathcal{S}^{p_1-2,p_2-1,p_3-1}_{\mathbf{r}_1-2,\mathbf{r}_2-1,\mathbf{r}_3-1} & \mathcal{S}^{p_1-2,p_2-2,p_3}_{\mathbf{r}_1-2,\mathbf{r}_2-2,\mathbf{r}_3} \end{pmatrix},$$

$$V^{3,2} = \begin{pmatrix} \mathcal{S}^{p_1-1,p_2-2,p_3-2}_{\mathbf{r}_1-1,\mathbf{r}_2-2,\mathbf{r}_3-2} \\ \mathcal{S}^{p_1-2,p_2-1,p_3-2}_{\mathbf{r}_1-2,\mathbf{r}_2-1,\mathbf{r}_3-2} \\ \mathcal{S}^{p_1-2,p_2-2,p_3-1}_{\mathbf{r}_1-2,\mathbf{r}_2-2,\mathbf{r}_3-1} \end{pmatrix}.$$

Finally, in the last row, we obtain the first three spaces by symmetry and derive the last one via the div operator:

$$V^{3,3} = \mathcal{S}^{p_1-2,p_2-2,p_3-2}_{\mathbf{r}_1-2,\mathbf{r}_2-2,\mathbf{r}_3-2}.$$

Now, we can define the elasticity complex (12) in three dimensions via the second and third rows of the diagram (46)

$$\begin{tikzcd} 0 \arrow[r] & V^{0,1} \arrow[r, "\mathrm{grad}"] & V^{1,1} \arrow[r, "\mathrm{curl}"] & V^{2,1} \arrow[r, "\mathrm{div}"] & V^{3,1} \arrow[r] & 0 \\ 0 \arrow[r] & V^{0,2} \arrow[r, "\mathrm{grad}"] \arrow[ur, "-\mathrm{mskw}"] & V^{1,2} \arrow[r, "\mathrm{curl}"] \arrow[ur, "\mathcal{T}"] & V^{2,2} \arrow[r, "\mathrm{div}"] \arrow[ur, "2\,\mathrm{vskw}"] & V^{3,2} \arrow[r] & 0. \end{tikzcd} \tag{50}$$

It is easy to check the relations such as $\mathrm{mskw}\, V^{0,2} \subset V^{1,1}$, $\mathcal{T} V^{1,2} = V^{2,1}$ (by definition), and $vskw(V^{2,2}) \subset V^{3,1}$. Therefore the diagram (50) satisfies all the assumptions for the BGG construction [10]. We can read out the 3D elasticity complex from the second and third rows of (46) as follows:

$$0 \longrightarrow V^{0,1} \xrightarrow{\text{def grad}} V^{1,1} \cap \mathbb{S} \xrightarrow{\text{inc}} V^{2,2} \cap \mathbb{S} \xrightarrow{\text{div}} V^{3,2} \longrightarrow 0, \tag{51}$$

Similarly, from the first and second rows of (46), we obtain the Hessian complex:

$$0 \longrightarrow V^{0,0} \xrightarrow{\text{hess}} V^{1,1} \cap \mathbb{S} \xrightarrow{\text{curl}} V^{2,1} \cap \mathbb{T} \xrightarrow{\text{div}} V^{3,1} \longrightarrow 0, \tag{52}$$

and from the third and fourth rows of (46), we obtain the div div complex:

$$0 \longrightarrow V^{0,2} \xrightarrow{\text{dev grad}} V^{1,2} \cap \mathbb{T} \xrightarrow{\text{sym curl}} V^{2,2} \cap \mathbb{S} \xrightarrow{\text{div div}} V^{3,3} \longrightarrow 0. \tag{53}$$

4. Finite element BGG complexes

Within this Section, we first present finite element (FE) de Rham complexes in 1D fulfilling Assumption 1. Later on, FE BGG complexes are introduced and the obtained results are compared to existing FEs in the literature.

4.1. **Finite elements in 1D.** When we turn from splines to FEs, the view changes from global to local. Again, we consider a subdivision of the interval of interest into subintervals. We define polynomial spaces on each subinterval by affine mapping of a polynomial space on the reference interval $[0,1]$ to the actual interval. What constituted the knot vector for splines are now the interfaces between the subintervals together with so-called node functionals, which are also defined by mapping from the reference interval. It is common standard to assume that continuity conditions between all subintervals are equal. Thus, a FE space is defined by

(1) The subdivision into subintervals
(2) The polynomial space and node functionals on the reference interval

Note that in one space dimension this corresponds to a spline space where each knot has the same multiplicity. In higher dimensions, the methods differ by the fact that the FE version does not require tensor product meshes, just each cell must be a tensor product.

Following these remarks, $\mathcal{S}_r^q(\mathcal{I})$ denotes the space of polynomials on the reference interval $\mathcal{I}$ of degree q equipped with node functionals which establish regularity of degree r at the interfaces between subintervals. In the examples below, $r=-1$ will refer to discontinuous FEs, $r=0$ to continuous, and $r=1$ to continuously differentiable elements.

We now derive the FE discretization for the one-dimensional BGG diagram (5) as well as the one-dimensional BGG complex (6). First, we observe that the regularity index of the last element in the complex is two less compared to the first element. As we cannot go below L^2, this implies that we must start with (at least) H^2 regularity on the left. The proxy field FE-BGG diagram reads:

$$\begin{tikzcd} 0 \arrow[r] & W^{0,0} \arrow[r, "\partial_x"] & W^{1,0} \arrow[r] & 0 \\ 0 \arrow[r] & W^{0,1} \arrow[r, "\partial_x"] \arrow[ur, "I"] & W^{1,1} \arrow[r] & 0. \end{tikzcd} \tag{54}$$

In detail, the spaces in the FE complex are (see [14, 13]):

- $W^{0,0}$ is the space of polynomials in $\mathcal{S}_{\mathbf{r}}^q(\mathcal{I})$ defined by a modified set of Hermite interpolation conditions ensuring continuously differentiable transitions to the neighboring intervals, complemented with a set of interior moments. This results in the following set of $q+1$ node functionals:

$$\mathcal{N}^{0,0}_{2i+1}(u) = \partial_x^{i+1}u(0), \quad \mathcal{N}^{0,0}_{2i+2}(u) = \partial_x^{i+1}u(1), \quad i=0,\dots,r-1, \tag{55}$$

$$\mathcal{N}^{0,0}_{2r+i}(u) = \int_0^1 \ell_{i-1}\partial_x u \,\mathrm{d}x, \quad i=1,\dots,q-2r, \tag{56}$$

$$\mathcal{N}^{0,0}_{q+1}(u) = u(1)+u(0), \tag{57}$$

where ℓ_i denotes the Legendre polynomial of degree i on the interval $[0,1]$, normalized with the condition $\ell_i(1)=1$.

- $W^{1,0}$ is the space of polynomials in $\mathcal{S}^{q-1}_{r-1}(\mathcal{I})$ equipped with the following set of q node functionals

$$\mathcal{N}^{1,0}_{2i+1}(v) = \partial^i_x v(0), \quad \mathcal{N}^{1,0}_{2i+2}(v) = \partial^i_x v(1), \quad i = 0, \dots, r-1, \tag{58}$$

$$\mathcal{N}^{1,0}_{2r+i}(v) = \int_0^1 \ell_{i-1} v \,\mathrm{d}x, \quad i = 1, \dots, q-2r. \tag{59}$$

- $W^{0,1}$ is the space of polynomials in $\mathcal{S}^{q-1}_{r-1}(\mathcal{I})$ equipped with the set of node functionals $\{\mathcal{N}^{0,1}_j\}_{j=1}^q$ defined as in (55)-(56)-(57) with r and q replaced by $r-1$ and $q-1$, respectively.
- $W^{1,1}$ is the space of polynomials in $\mathcal{S}^{q-2}_{r-2}(\mathcal{I})$ equipped with the set of node functionals $\{\mathcal{N}^{1,1}_j\}_{j=1}^{q-1}$ defined as in (58)-(59) with r and q replaced by $r-1$ and $q-1$, respectively.

It is easily verified that each row in (54) forms a complex and ∂_x is onto, so that Assumption 1 is satisfied.

Let $n_{k,l}$ be the dimension of the shape function space $W^{k,l}$. Given the above-mentioned node functionals, we can introduce the corresponding dual basis functions $\{\psi^{k,l}_i\}_{i=1,\dots,n_{k,l}}$ for $W^{k,l}$, fulfilling

$$\mathcal{N}^{k,l}_j(\psi^{k,l}_i) = \delta_{ij}, \qquad k,l = 0,1,$$

for all admissible values of i and j. Then, the canonical interpolation operators on the polynomial spaces are defined on the reference interval as

$$\Pi^{k,l}(u) := \sum_{i=1}^{n_{k,l}} \mathcal{N}^{k,l}_i(u)\psi^{k,l}_i. \tag{60}$$

The basis functions $\{\psi^{k,l}_i\}$ together with the node functionals $\{\mathcal{N}^{k,l}_i\}$ for $k,l = 0,1$ and all admissible values of i, fulfill the assumptions of the commuting Lemma 2 in [13]. Hence, the canonical interpolation operators (60) commute with the derivative, i.e., for all $u \in C^\infty(\mathcal{I})$, there holds

$$\partial_x \Pi^{0,l} u = \Pi^{1,l}\partial_x u, \qquad l = 0,1.$$

Lemma 5. *The canonical interpolation operator commutes with the identity operator in* (54)*, that is, for any $u \in C^1(\mathcal{I})$ there holds*

$$\Pi^{0,1}u = \Pi^{1,0}u. \tag{61}$$

Proof. First, we observe that the node functionals in (56) for $i > 1$ can be transformed by integration by parts into linear combinations of those in (59). In the case $i = 1$ they simply reduce to the difference of the values in the end points. Thus, the sets of node functionals for $W^{1,0}$ and for $W^{0,1}$ can each be obtained as linear combinations of the other set. We decompose

$$C^\infty = \mathbb{P}_{q-1} \oplus \mathbb{P}^\perp_{q-1}, \tag{62}$$

where $\mathbb{P}_{q-1}^{\perp}$ is the polar set of the node functionals, namely

$$\mathbb{P}_{q-1}^{\perp} = \{u \in C^\infty \mid \mathcal{N}_i^{1,0}(u) = 0,\ i = 1, \dots, q\} \tag{63}$$

$$= \{u \in C^\infty \mid \mathcal{N}_i^{0,1}(u) = 0,\ i = 1, \dots, q\}. \tag{64}$$

Hence, decomposing $u \in C^\infty$ according to this direct sum as $u = p + u^\perp$ and exploiting that both interpolation operators are projections onto $\mathbb{P}_{q-1}$, there holds

$$\Pi^{0,1} u = \Pi^{0,1} p = p = \Pi^{1,0} p = \Pi^{1,0} u. \tag{65}$$

□

The node functionals $\{\mathcal{N}_i^{k,l}\}$ are well-defined for smooth functions. However, as outlined in Remark 3 in [13], weighted node functionals $\{\overline{\mathcal{N}}_i^{k,l}\}$ can be employed to obtain an L^2-bounded quasi-interpolation operator

$$\widetilde{\pi}^{k,l}(u) := \sum_{i=1}^{n_{k,l}} \overline{\mathcal{N}}_i^{k,l}(u) \psi_i^{k,l}, \qquad k, l = 0, 1, \qquad u \in L^2(I), \tag{66}$$

which commutes with the exterior derivative. We recall that $\widetilde{\pi}^{k,l}$ is obtained by averaging over canonical interpolation operators (60) on perturbed intervals. Since (61) holds for each of them, and the averaging weights are chosen consistently, we conclude that the quasi-interpolation operators $\widetilde{\pi}^{k,l}$ commute with the operators $S^{k,l}$. Hence, they satisfy Assumption 2. Note that applying Schöberl's trick, see for instance section 5.3 in [14], we can even obtain a projection onto the discrete space.

4.2. **Finite elements in three dimensions.** Tensor products of one-dimensional functions are simply defined as $[u \otimes v](x, y) = u(x)v(y)$. Functions of this type are also called rank-1 tensors. Since rank-1 tensors form a basis of the tensor product space, it is sufficient to define the tensor product of node functionals on such tensors and then extend them by linearity to the whole space. Let for instance $\mathcal{N}_1$ and $\mathcal{N}_2$ be node functionals in one dimension. Then $[\mathcal{N}_1 \otimes \mathcal{N}_2](u \otimes v) = \mathcal{N}_1(u)\mathcal{N}_2(v)$. Choosing node functionals $\mathcal{N}_1(u) = u'(0)$, $\mathcal{N}_2(u) = u(0)$, and $\mathcal{N}_3(u) = \int u \, \mathrm{d}x$ we obtain by this construction in two dimensions

$$\begin{aligned}
&[\mathcal{N}_1 \otimes \mathcal{N}_1](f) = \partial_{xy} f(0, 0), \qquad && [\mathcal{N}_1 \otimes \mathcal{N}_3](f) = \int_0^1 \partial_x f(0, y)\, dy, \\
&[\mathcal{N}_1 \otimes \mathcal{N}_2](f) = \partial_x f(0, 0), && [\mathcal{N}_2 \otimes \mathcal{N}_3](f) = \int_0^1 f(0, y)\, dy, \\
&[\mathcal{N}_2 \otimes \mathcal{N}_1](f) = \partial_y f(0, 0), && [\mathcal{N}_3 \otimes \mathcal{N}_3](f) = \int_0^1 f(x, y)\, dx\, dy.
\end{aligned} \tag{67}$$

The three-dimensional construction is analogous, such that we only show the generic two-dimensional case here.

Now we have set the stage for studying specific FEs for BGG complexes. Let us begin with the lowest regularity ($r = 1$) element family for the div div complex obtained by our method. This complex combines the last two rows of the diagram (46). Starting with $V^{3,3}$, we chose $\mathbf{r}_1 = \mathbf{r}_2 = \mathbf{r}_3 = 1$ to obtain an L^2-conforming space. Focusing on the isotropic case $p_1 = p_2 = p_3 = p$, we obtain the following polynomial spaces for the div div complex:

(68)

$$V^{0,2} = \begin{pmatrix} \mathcal{S}^{p,p-1,p-1}_{1,0,0} \\ \mathcal{S}^{p-1,p,p-1}_{0,1,0} \\ \mathcal{S}^{p-1,p-1,p}_{0,0,1} \end{pmatrix} \quad V^{1,2} = \begin{pmatrix} \mathcal{S}^{p-1,p-1,p-1}_{0,0,0} & \mathcal{S}^{p,p-2,p-1}_{1,-1.0} & \mathcal{S}^{p,p-1,p-2}_{1,0,-1} \\ \mathcal{S}^{p-2,p,p-1}_{-1,1,0} & \mathcal{S}^{p-1,p-1,p-1}_{0,0,0} & \mathcal{S}^{p-1,p,p-2}_{0,1,-1} \\ \mathcal{S}^{p-2,p-1,p}_{-1,0,1} & \mathcal{S}^{p-1,p-2,p}_{0,-1,1} & \mathcal{S}^{p-1,p-1,p-1}_{0,0,0} \end{pmatrix}$$

(69)

$$V^{3,3} = \mathcal{S}^{p-2,p-2,p-2}_{-1,-1,-1} \qquad V^{2,2} = \begin{pmatrix} \mathcal{S}^{p,p-2,p-2}_{1,-1,-1} & \mathcal{S}^{p-1,p-1,p-2}_{0,0,-1} & \mathcal{S}^{p-1,p-2,p-1}_{0,-1,0} \\ \mathcal{S}^{p-1,p-1,p-2}_{0,0,-1} & \mathcal{S}^{p-2,p,p-2}_{-1,1,-1} & \mathcal{S}^{p-2,p-1,p-1}_{-1,0,0} \\ \mathcal{S}^{p-1,p-2,p-1}_{0,-1,0} & \mathcal{S}^{p-2,p-1,p-1}_{-1,0,0} & \mathcal{S}^{p-2,p-2,p}_{-1,-1,1} \end{pmatrix}$$

Thus, we have obtained exactly the same polynomial spaces as [40] as a special case of our theory. In particular, the three spaces on the diagonal of $V^{1,2}$ are identical, thus facilitating trace free matrices. Similarly, $V^{2,2}$ is suitable for symmetric matrices.

The degrees of freedom of these spaces can be read from the lower indices and can be constructed by tensor products as in equation (67). Beginning from the right, $V^{3,3}$ is simply the space of discontinuous tensor product polynomials $\mathbb{Q}_{p-2}$ with only volume node functionals, implemented as moments with respect to the same space,

$$\int_K p\phi \, \mathrm{d}x \qquad\qquad \phi \in \mathbb{Q}_{p-2}(K).$$

For $V^{2,2}$, the div div-conforming space of symmetric matrices, we obtain for the diagonal element σ_{ii} the conditions, that the piecewise polynomials are continuously differentiable in x_i-direction and discontinuous in the other two coordinate directions. Thus, we introduce the set of node functionals

$$\int_F (n^T \sigma n)\phi \, \mathrm{d}s \qquad\qquad \phi \in \mathbb{Q}_{p-2}(F), \tag{70}$$

$$\int_F (n^T \partial_n \sigma n)\phi \, \mathrm{d}s \qquad\qquad \phi \in \mathbb{Q}_{p-2}(F), \tag{71}$$

where F runs through all faces of the reference cube K. Here, we used that on each Cartesian face, $n^T\sigma n$ selects the diagonal element σ_{ii} where the unit vector e_i is orthogonal to F. These degrees of freedom are shown for the lowest order case in the top row of figure 1. For visualization purposes, the moments on faces are displayed as equivalent values in quadrature points. At the bottom of figure 1, we show how the degrees of freedom for the off-diagonal elements are constructed as tensor products of their one-dimensional fibers in the lowest order case.

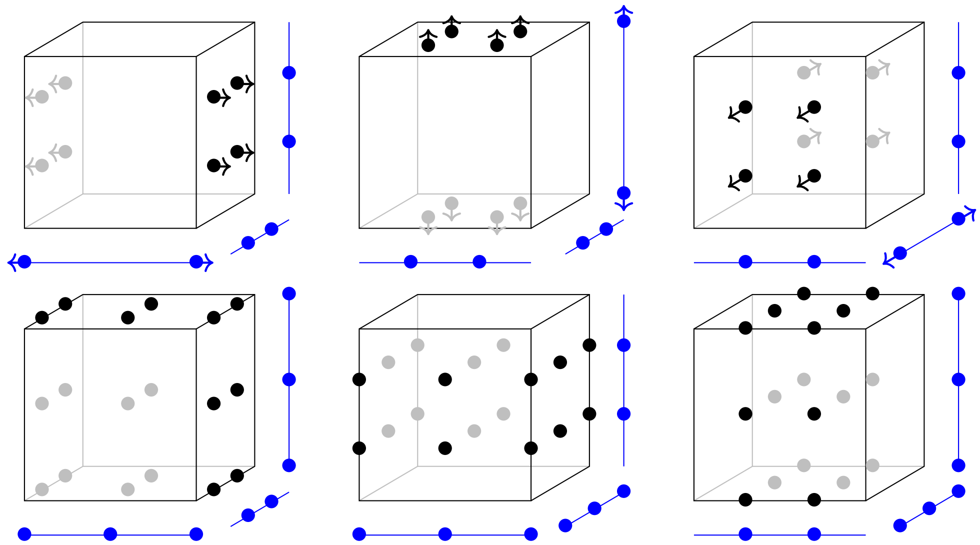

FIGURE 1. The degrees of freedom of the lowest order version of the div div-conforming space $V^{2,2}$ and the fibers of the tensor products in blue. Top row the diagonal entries $\sigma_{11}, \sigma_{22}, \sigma_{33}$. Bottom row $\sigma_{12} = \sigma_{21}$, $\sigma_{13} = \sigma_{31}$, and $\sigma_{23} = \sigma_{32}$. Dots indicate function values, arrows indicate directional derivatives. Moments are visualized by quadrature points.

The diagonal elements of a tensor σ in the space $V^{1,2}$ are each from the standard continuous, isotropic FE space $\mathbb{Q}_{p-1}$. The off-diagonal entries are anisotropic in polynomial degree and degrees of freedom. Instead of writing down complicated formulas for node values and test spaces, we show their construction in the lowest order case in figure 2. Each of the entries is a tensor product of a polynomial of degree 3, one of degree 2 and one of degree 1, and the six off-diagonal entries traverse all possible combinations of these. The node functionals are those of Hermite and Lagrange interpolation, respectively.

The tensor product construction also yields FEs for the elasticity complex. The degrees of freedom of the lowest order strain element of our construction is displayed in figure 3. The corresponding stress element is $V^{2,2}$ in figure 1. Comparing to [41], we see that their element in our notation is

$$V^{2,2}_{\mathrm{HMZ}} = \begin{pmatrix} \mathcal{S}^{2,0,0}_{0,-1,-1} & \mathcal{S}^{1,1,0}_{0,0,-1} & \mathcal{S}^{1,0,1}_{0,-1,0} \\ \mathcal{S}^{1,1,0}_{0,0,-1} & \mathcal{S}^{0,2,0}_{-1,0,-1} & \mathcal{S}^{0,1,1}_{-1,0,0} \\ \mathcal{S}^{1,0,1}_{0,-1,0} & \mathcal{S}^{0,1,1}_{-1,0,0} & \mathcal{S}^{0,0,2}_{-1,-1,0} \end{pmatrix}, \quad V^{3,2}_{\mathrm{HMZ}} = \begin{pmatrix} \mathcal{S}^{1,0,0}_{-1,-1,-1} \\ \mathcal{S}^{0,1,0}_{-1,-1,-1} \\ \mathcal{S}^{0,0,1}_{-1,-1,-1} \end{pmatrix}. \tag{72}$$

Thus, the polynomial spaces of their element correspond to the polynomial spaces in our construction with $p_1 = p_2 = p_3 = 2$, in which case we cannot use Hermitian degrees of freedom. Furthermore, we cannot fit the element

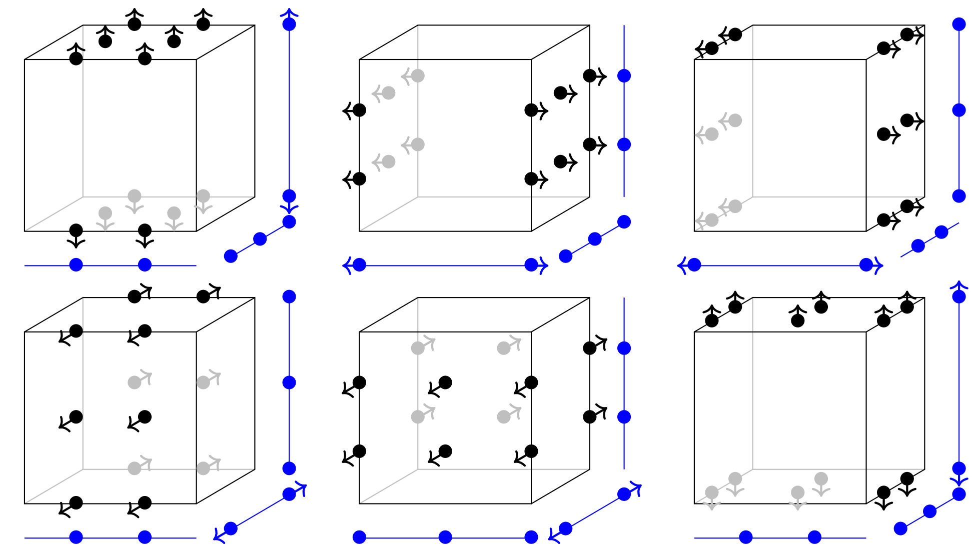

FIGURE 2. The degrees of freedom of the lowest order version of the symcurl-conforming space $V^{1,2}$ and the fibers of the tensor products in blue. First row for entries $\sigma_{21}, \sigma_{12}, \sigma_{13}$ and second row for $\sigma_{31}, \sigma_{32}, \sigma_{32}$. Dots indicate function values, arrows indicate directional derivatives. Moments are visualized by quadrature points.

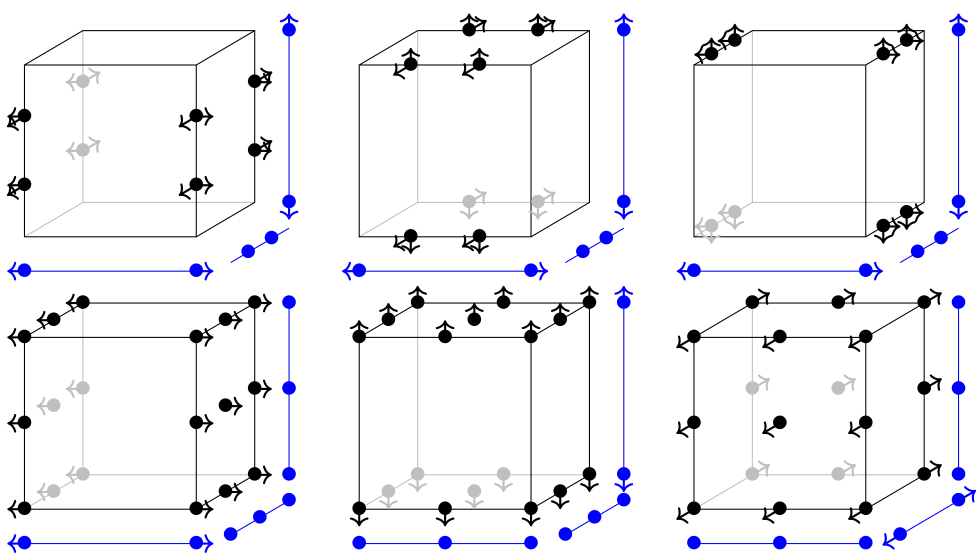

FIGURE 3. Degrees of freedom for the lowest order strain element $V^{1,1}$ of the elasticity complex. Diagonal entries $\sigma_{11}, \sigma_{22}, \sigma_{33}$ in the top row. Off-diagonal entries $\sigma_{23} = \sigma_{32}$, $\sigma_{13} = \sigma_{31}$, and $\sigma_{12} = \sigma_{21}$ in the bottom row. Pairs of arrows indicate first order and mixed second order derivatives.

into the full four row diagram (46) as the space $V_{\text{HMZ}}^{2,2}$ is not the range of a curl. Accordingly, the regularity indices do not fit into our construction. The spaces for off-diagonal matrix entries exhibit more regularity than expected, but the divergence operator is onto, since the diagonal elements have the right regularity. Hence, we conclude that pairs in the BGG complex can be constructed in a more general way than our construction, but that this typically may not yield a whole FE complex with locally defined degrees of freedom.

5. Conclusions

We presented a general construction of Bernstein-Gelfand-Gelfand (BGG) complexes by tensor products of piecewise polynomial spaces. The construction is based on merging two complexes of alternating forms of arbitrary degrees in $\mathbb{R}^n$ via cross-linking maps which commute with the differential operators of the complexes to obtain a single BGG complex. We first constructed the BGG complexes in one-dimension, then extended our construction to n-dimensions via the tensor product of spaces and the interpolation operators.

The method is based on scales of one-dimensional piecewise polynomial spaces characterized abstractly by their polynomial degree and smoothness parameter. Under the assumption of a commutativity between the interpolation operator of these spaces and the operators in the one-dimensional BGG diagram, we derived BGG complexes in any dimension with commuting interpolation operators.

We presented two examples for the application of this construction. For once, standard spline spaces in one dimension can be employed to generate the BGG spline complexes. Then, we presented the same construction for finite element spaces and showed their degrees of freedom in three dimensions.

Nevertheless, the construction for some more delicate BGG complexes remains open. We take the conformal deformation complex [10, (50)] as an example:

$$\begin{aligned} 0 \longrightarrow H^q \otimes \mathbb{V} &\xrightarrow{\operatorname{dev}\operatorname{def}} H^{q-1} \otimes (\mathbb{S} \cap \mathbb{T}) \\ &\xrightarrow{\quad\operatorname{cot}\quad} H^{q-4} \otimes (\mathbb{S} \cap \mathbb{T}) \xrightarrow{\operatorname{div}} H^{q-5} \otimes \mathbb{V} \longrightarrow 0. \end{aligned} \tag{73}$$

Here $\operatorname{dev}\operatorname{def} = \operatorname{dev}\operatorname{sym}\operatorname{grad}$ is the symmetric trace-free part of the gradient, and $\operatorname{cot} := \operatorname{curl}\mathcal{T}^{-1}\operatorname{curl}\mathcal{T}^{-1}\operatorname{curl}$ leads to the linearized Cotton-York tensor with modified trace. If the vector element on the left has tensor polynomial structure like

$$\omega = \begin{pmatrix} p_1, q_1, r_1 \\ p_2, q_2, r_2 \\ p_3, q_3, r_3 \end{pmatrix}, \tag{74}$$

in order to be symmetric and trace free, we look at the orders of the gradient

$$\nabla\omega = \begin{pmatrix} p_1-1, q_1, r_1 & p_1, q_1-1, r_1 & p_1, q_1, r_1-1 \\ p_2-1, q_2, r_2 & p_2, q_2-1, r_2 & p_2, q_2, r_2-1 \\ p_3-1, q_3, r_3 & p_3, q_3-1, r_3 & p_3, q_3, r_3-1 \end{pmatrix}. \tag{75}$$

For instance, in order to be symmetric, we must require $p_1 = p_2 - 1$, but for the trace adding up to zero, we need $p_2 = p_1 - 1$.

Based on the construction in this paper, one may further investigate numerical schemes in the direction of isogeometric analysis, c.f., [2, 34, 43, 49].

Appendix A. Proxy fields

When discussing concrete realizations of the diagram (24) in spline and finite element spaces below, we will define them in terms of proxy fields for the differential forms involved. Thus, we need vector representations of alternating forms. In three dimensions, we can choose the basis dx_1, dx_2, dx_3 for $\mathrm{Alt}^{0,1} \cong \mathrm{Alt}^1$ and $\mathrm{Alt}^{1,0} \cong \mathrm{Alt}^1$. Thus, we obtain a basis for the according vector space by assigning $e_i = dx_i$ for $i = 1, 2, 3$. For the spaces $\mathrm{Alt}^{0,2}$ and $\mathrm{Alt}^{2,0}$, we assign in similar fashion

$$e_1 = dx_2 \wedge dx_3, \quad e_2 = dx_3 \wedge dx_1, \quad e_3 = dx_1 \wedge dx_2. \tag{76}$$

The space $\mathrm{Alt}^{1,1} = \mathrm{Alt}^1 \otimes \mathrm{Alt}^1$ consists of matrices spanned by the basis $e_{ij} = dx_i \otimes dx_j$ for $i, j = 1, 2, 3$. A basis for $\mathrm{Alt}^{1,2} = \mathrm{Alt}^1 \otimes \mathrm{Alt}^2$ can be formed of elements

$$e_{i,1} = dx_i \otimes dx_2 \wedge dx_3, \quad e_{i,2} = dx_i \otimes dx_3 \wedge dx_1, \quad e_{i,3} = dx_i \otimes dx_1 \wedge dx_2, \qquad i = 1, 2, 3. \tag{77}$$

Following [10], we introduce notation for the algebraic operations we need in this picture. Now we consider the following basic linear algebraic operations: $\mathrm{skw} : \mathbb{M} \to \mathbb{K}$ and $\mathrm{sym} : \mathbb{M} \to \mathbb{S}$ are the skew and symmetric part operators; $\mathrm{tr} : \mathbb{M} \to \mathbb{R}$ is the matrix trace; $\iota : \mathbb{R} \to \mathbb{M}$ is the map $\iota u := uI$ identifying a scalar with a scalar matrix; $\mathrm{dev} : \mathbb{M} \to \mathbb{T}$ given by $\mathrm{dev} w := w - 1/n\,\mathrm{tr}(w)I$ is the deviator, or trace-free part. In three space dimensions, we can identify a skew symmetric matrix with a vector,

$$\mathrm{mskw}\begin{pmatrix} v_1 \\ v_2 \\ v_3 \end{pmatrix} := \begin{pmatrix} 0 & -v_3 & v_2 \\ v_3 & 0 & -v_1 \\ -v_2 & v_1 & 0 \end{pmatrix}.$$

Consequently, we have $\mathrm{mskw}(v)w = v \times w$ for $v, w \in \mathbb{V}$, where $v \times w$ denotes the cross product between $v = (v_1, v_2, v_3)$ and $w = (w_1, w_2, w_3)$ defined as

$$v \times w = \left| \begin{pmatrix} e_1 & e_2 & e_3 \\ v_1 & v_2 & v_3 \\ w_1 & w_2 & w_3 \end{pmatrix} \right|,$$

$\{e_j\}_{j=1,2,3}$ denoting the standard basis of $\mathbb{R}^3$. Using the same notation as in 3D, we define $\mathrm{mskw} : \mathbb{R} \to \mathbb{K}$ in two-dimensions by

$$\mathrm{mskw}(u) := \begin{pmatrix} 0 & u \\ -u & 0 \end{pmatrix} \quad \text{in } \mathbb{R}^2.$$

We also define the operators

$$\begin{aligned} \mathrm{vskw}\colon \mathbb{M} \to \mathbb{V} \qquad & \qquad \mathrm{vskw} = \mathrm{mskw}^{-1} \circ \mathrm{skw} \\ \mathcal{T}\colon \mathbb{M} \to \mathbb{M} \qquad & \qquad \mathcal{T}u = u^T - \mathrm{tr}(u) I. \end{aligned}$$

Appendix B. Characterization of s operators

In this appendix, we prove equation (8), containing the expression of $s^{i,j}$ applied to a basis. We first recall, [7, Equation (2.1)], which will be helpful below:

$$[dx^1 \wedge \cdots \wedge dx^k](u_1, \cdots, u_k) = \sum_{l=1}^{k} (-1)^{l+1} dx^1(u_l) [dx^2 \wedge \cdots \wedge dx^k](u_1, \cdots, \widehat{u_l}, \cdots, u_k). \tag{78}$$

Lemma 6. *Let $\sigma \in \Sigma(k,n)$ and $\tau \in \Sigma(m,n)$. Then*

$$s^{k,m}(dx^\sigma \otimes dx^\tau) = \sum_{l=1}^{m} (-1)^{l-1} dx^{\tau_l} \wedge dx^\sigma \otimes dx^{\tau_1} \wedge \cdots \wedge \widehat{dx^{\tau_l}} \wedge \cdots \wedge dx^{\tau_m}. \tag{79}$$

Let $\boldsymbol{s} \in X_k$ and $\boldsymbol{t} \in X_m$ be the characteristic vectors of σ and τ, respectively. Then, equation (79) can be equivalently written as

$$\begin{aligned} & s^{k,m}\big((dx^1)^{s_1} \wedge \cdots \wedge (dx^n)^{s_n} \otimes (dx^1)^{t_1} \wedge \cdots \wedge (dx^n)^{t_n}\big) \\ & \quad = \sum_{l=1}^{n} (-1)^{|\boldsymbol{t}|_l + 1} \delta_{1,t_l} dx^l \wedge (dx^1)^{s_1} \wedge \cdots \wedge (dx^n)^{s_n} \otimes \cdots \\ & \qquad\qquad (dx^1)^{t_1} \wedge \cdots \wedge \widehat{dx^l} \wedge \cdots \wedge (dx^n)^{t_n}. \end{aligned} \tag{80}$$

Proof. Let $\sigma \in \Sigma(k,n)$ and let $\tau \in \Sigma(m,n)$. By the definition of $s^{k,m}$ in equation (7), there holds

$$\begin{aligned} T_1 &:= s^{k,m}[dx^\sigma \otimes dx^\tau](e_{\mathbf{r}_1}, \ldots, e_{\mathbf{r}_{k+1}})(e_{\beta_1}, \ldots, e_{\beta_{m-1}}) \\ &= \sum_{\ell=1}^{k+1} (-1)^{\ell+1} [dx^\sigma \otimes dx^\tau](e_{\mathbf{r}_1}, \ldots, \widehat{e_{\mathbf{r}_\ell}}, \ldots, e_{\mathbf{r}_{k+1}})(e_{\mathbf{r}_\ell}, e_{\beta_1}, \ldots, e_{\beta_{m-1}}) \\ &= \sum_{\ell=1}^{k+1} (-1)^{\ell+1} dx^\sigma(e_{\mathbf{r}_1}, \ldots, \widehat{e_{\mathbf{r}_\ell}}, \ldots, e_{\mathbf{r}_{k+1}}) dx^\tau(e_{\mathbf{r}_\ell}, e_{\beta_1}, \ldots, e_{\beta_{m-1}}), \end{aligned}$$

for $\mathbf{r} \in \Sigma(k+1,n)$ and $\beta \in \Sigma(m-1,n)$. We observe that at most one term in the sum on the right is nonzero, namely where ℓ can be chosen such there holds

$$\{\mathbf{r}_1,\dots,\mathbf{r}_{k+1}\} = \{\mathbf{r}_\ell,\sigma_1,\dots,\sigma_k\}, \qquad \{\mathbf{r}_\ell,\beta_1,\dots,\beta_{m-1}\} = \{\tau_1,\dots,\tau_m\}. \tag{81}$$

In particular, we note that $\mathbf{r}_\ell \neq \sigma_i$ for $i = 1,\dots,k$ and there is an index j such that $\mathbf{r}_\ell = \tau_j$. Define $\tau' \in \Sigma(m-1,n)$ by removing τ_j from τ. Then, by (78),

$$\begin{aligned} dx^\tau(e_{\mathbf{r}_\ell}, e_{\beta_1},\dots,e_{\beta_{m-1}}) &= (-1)^{j+1}[dx^{\tau_j}\wedge dx^{\tau'}](e_{\mathbf{r}_\ell}, e_{\beta_1},\dots,e_{\beta_{m-1}}) \\ &= (-1)^{j+1} dx^{\tau_j}(e_{\mathbf{r}_\ell}) dx^{\tau'}(e_{\beta_1},\dots,e_{\beta_{m-1}}) \\ &= (-1)^{j+1} dx^{\tau'}(e_{\beta_1},\dots,e_{\beta_{m-1}}). \end{aligned}$$

Thus,

$$T_1 = (-1)^{\ell+j}\delta_{\mathbf{r}_\ell,\tau_j} dx^\sigma(e_{\mathbf{r}_1},\dots,\widehat{e_{\mathbf{r}_\ell}},\dots,e_{\mathbf{r}_{k+1}}) dx^{\tau'}(e_{\beta_1},\dots,e_{\beta_{m-1}}). \tag{82}$$

Next, we start from (79) and let (again using τ' for τ without τ_j)

$$\begin{aligned} T_2 &:= \sum_{j=1}^m (-1)^{j+1}\left[dx^{\tau_j}\wedge dx^\sigma \otimes dx^{\tau'}\right](e_{\mathbf{r}_1},\dots,e_{\mathbf{r}_{k+1}})(e_{\beta_1},\dots,e_{\beta_{m-1}}) \\ &= \sum_{j=1}^m (-1)^{j+1}\left[dx^{\tau_j}\wedge dx^\sigma\right](e_{\mathbf{r}_1},\dots,e_{\mathbf{r}_{k+1}}) dx^{\tau'}(e_{\beta_1},\dots,e_{\beta_{m-1}}). \end{aligned}$$

The last sum contains at most one nonzero term, namely if j can be chosen such that there holds

$$\{\tau_j,\beta_1,\dots,\beta_{m-1}\} = \{\tau_1,\dots,\tau_m\}, \qquad \{\mathbf{r}_1,\dots,\mathbf{r}_{k+1}\} = \{\tau_j,\sigma_1,\dots,\sigma_k\}. \tag{83}$$

Since $\mathbf{r}_1,\dots,\mathbf{r}_{k+1}$ is as in (82), the index not contained in σ is $\mathbf{r}_\ell$. By (78) we get

$$[dx^{\tau_j}\wedge dx^\sigma](e_{\mathbf{r}_1},\dots,e_{\mathbf{r}_{k+1}}) = (-1)^{\ell+1} dx^{\tau_j}(e_{\mathbf{r}_\ell}) dx^\sigma(e_{\mathbf{r}_1},\dots,\widehat{e_{\mathbf{r}_\ell}},\dots,e_{\mathbf{r}_{k+1}}). \tag{84}$$

Summarizing, we obtain

$$T_2 = (-1)^{\ell+j}\delta_{\mathbf{r}_\ell,\tau_j} dx^\sigma(e_{\mathbf{r}_1},\dots,\widehat{e_{\mathbf{r}_\ell}},\dots,e_{\mathbf{r}_{k+1}}) dx^{\tau'}(e_{\beta_1},\dots,e_{\beta_{m-1}}), \tag{85}$$

which is equal to T_1 in (82). $\square$

We give a simple example to illustrate the lemma. For $k = m = 1$, consider $s^{1,1}[dx^1\otimes dx^2](e_1,e_2)()$, where e_i is the dual basis of dx^i, $i = 1,2$. By definition of s, we have that the above is equal to

$$[dx^1\otimes dx^2](e_2)(e_1) - [dx^1\otimes dx^2](e_1)(e_2) = -1.$$

By Lemma 6, the above is equal to

$$2\big[[dx^2\wedge dx^1]\otimes 1 - [dx^1\wedge dx^2]\otimes 1\big](e_1,e_2) = 2\cdot(0-\frac{1}{2}) = -1.$$

References

1. Arzhang Angoshtari and Arash Yavari, *Differential complexes in continuum mechanics*, Archive for Rational Mechanics and Analysis **216** (2015), no. 1, 193–220.
2. Jeremias Arf and Bernd Simeon, *Mixed isogeometric discretizations for planar linear elasticity*, arXiv preprint arXiv:2204.08095 (2022).
3. ______, *Structure-preserving discretization of the hessian complex based on spline spaces*, arXiv preprint arXiv:2109.05293 (2021).
4. Douglas N. Arnold, *Finite Element Exterior Calculus*, Society for Industrial and Applied Mathematics, Philadelphia, PA, 2018.
5. Douglas N Arnold, Daniele Boffi, and Francesca Bonizzoni, *Finite element differential forms on curvilinear cubic meshes and their approximation properties*, Numerische Mathematik **129** (2015), no. 1, 1 – 20.
6. Douglas N. Arnold, Richard S. Falk, and Ragnar Winther, *Differential complexes and stability of finite element methods II: The elasticity complex*, Compatible Spatial Discretizations (D. Arnold, P. Bochev, R. Lehoucq, R. Nicolaides, and M. Shashkov, eds.), IMA Vol. Math. Appl., vol. 142, Springer, Berlin, 2006, pp. 47–68.
7. Douglas N Arnold, Richard S Falk, and Ragnar Winther, *Finite element exterior calculus, homological techniques, and applications*, Acta Numerica **15** (2006), 1–155.
8. ______, *Mixed finite element methods for linear elasticity with weakly imposed symmetry*, Mathematics of Computation **76** (2007), no. 260, 1699–1723.
9. ______, *Finite element exterior calculus: from Hodge theory to numerical stability*, Bulletin of the American Mathematical Society **47** (2010), no. 2, 281–354.
10. Douglas N Arnold and Kaibo Hu, *Complexes from complexes*, Foundations of Computational Mathematics **21** (2021), no. 6, 1739–1774.
11. Douglas N Arnold and Anders Logg, *Periodic table of the finite elements*, Siam News **47** (2014), no. 9, 212.
12. Douglas N Arnold and Ragnar Winther, *Mixed finite elements for elasticity*, Numerische Mathematik **92** (2002), no. 3, 401–419.
13. Francesca Bonizzoni and Guido Kanschat, *A tensor-product finite element cochain complex with arbitrary continuity*, ECCOMAS 2022. Available at `https://www.scipedia.com/public/Bonizzoni_Kanschat_2022a` (2022).
14. ______, *H^1-conforming finite element cochain complexes and commuting quasi-interpolation operators on Cartesian meshes*, Calcolo **58** (2021), no. 2, 1–29.
15. Annalisa Buffa, Judith Rivas, Giancarlo Sangalli, and Rafael Vázquez, *Isogeometric discrete differential forms in three dimensions*, SIAM Journal on Numerical Analysis **49** (2011), no. 2, 818–844.
16. Andreas Čap and Kaibo Hu, *BGG sequences with weak regularity and applications*, arXiv preprint arXiv:2203.01300 (2022).
17. Andreas Cap and Jan Slovák, *Parabolic geometries I*, Mathematical Surveys and Monographs, no. 154, American Mathematical Soc., 2009.
18. Andreas Čap, Jan Slovák, and Vladimír Souček, *Bernstein-Gelfand-Gelfand sequences*, Annals of Mathematics **154** (2001), no. 1, 97–113.
19. Long Chen and Xuehai Huang, *Discrete Hessian complexes in three dimensions*, arXiv preprint arXiv:2012.10914 (2020).
20. ______, *A finite element elasticity complex in three dimensions*, arXiv preprint arXiv:2106.12786 (2021).
21. ______, *Finite elements for divdiv-conforming symmetric tensors*, arXiv preprint arXiv:2005.01271 (2020).
22. ______, *Finite elements for divdiv-conforming symmetric tensors in arbitrary dimension*, arXiv preprint arXiv:2106.13384 (2021).
23. ______, *Geometric decompositions of div-conforming finite element tensors*, arXiv preprint arXiv:2112.14351 (2021).

24. Snorre H Christiansen, *Foundations of finite element methods for wave equations of Maxwell type*, pp. 335–393, Springer Berlin Heidelberg, 2009.
25. Snorre H Christiansen, Jay Gopalakrishnan, Johnny Guzmán, and Kaibo Hu, *A discrete elasticity complex on three-dimensional Alfeld splits*, arXiv preprint arXiv:2009.07744 (2020).
26. Snorre H Christiansen, Jun Hu, and Kaibo Hu, *Nodal finite element de Rham complexes*, Numerische Mathematik **139** (2018), no. 2, 411–446.
27. Snorre H Christiansen and Kaibo Hu, *Finite element systems for vector bundles: elasticity and curvature*, Foundations of Computational Mathematics (2022), 1–52.
28. Snorre H Christiansen, Kaibo Hu, and Espen Sande, *Poincaré path integrals for elasticity*, Journal de Mathématiques Pures et Appliquées **135** (2020), 83–102.
29. Martin Costabel and Alan McIntosh, *On Bogovskiĭ and regularized Poincaré integral operators for de Rham complexes on Lipschitz domains*, Mathematische Zeitschrift **265** (2010), no. 2, 297–320.
30. J Austin Cottrell, Thomas JR Hughes, and Yuri Bazilevs, *Isogeometric analysis: toward integration of CAD and FEA*, John Wiley & Sons, 2009.
31. L Beirao Da Veiga, Annalisa Buffa, Giancarlo Sangalli, and Rafael Vázquez, *Mathematical analysis of variational isogeometric methods*, Acta Numerica **23** (2014), 157–287.
32. Carl de Boor, *On calculating with b-splines*, Journal of Approximation Theory **6** (1972), 50–62.
33. Michael Eastwood, *A complex from linear elasticity*, Proceedings of the 19th Winter School" Geometry and Physics", Circolo Matematico di Palermo, 2000, pp. 23–29.
34. John A Evans, Michael A Scott, Kendrick M Shepherd, Derek C Thomas, and Rafael Vázquez Hernández, *Hierarchical B-spline complexes of discrete differential forms*, IMA Journal of Numerical Analysis **40** (2020), no. 1, 422–473.
35. Richard S Falk and Ragnar Winther, *The Bubble Transform and the de Rham Complex*, arXiv preprint arXiv:2111.08123 (2021).
36. Michael S Floater and Kaibo Hu, *A characterization of supersmoothness of multivariate splines*, Advances in Computational Mathematics **46** (2020), no. 5, 1–15.
37. Wolfgang Hackbusch, *Numerical tensor calculus*, Acta numerica **23** (2014), 651–742.
38. Jun Hu and Yizhou Liang, *Conforming discrete Gradgrad-complexes in three dimensions*, Mathematics of Computation **90** (2021), no. 330, 1637–1662.
39. Jun Hu, Yizhou Liang, and Rui Ma, *Conforming finite element DIVDIV complexes and the application for the linearized Einstein-Bianchi system*, arXiv preprint arXiv:2103.00088 (2021).
40. Jun Hu, Yizhou Liang, Rui Ma, and Min Zhang, *New conforming finite element divdiv complexes in three dimensions*, arXiv preprint arXiv:2204.07895 (2022).
41. Jun Hu, Hongying Man, and Shangyou Zhang, *A simple conforming mixed finite element for linear elasticity on rectangular grids in any space dimension*, J. Sci. Comput. **58** (2014), no. 2, 367–379.
42. Kaibo Hu, *Oberwolfach report: Discretization of hilbert complexes*, arXiv preprint arXiv:2208.03420 (2022).
43. Bernard Kapidani and Rafael Vázquez, *High order geometric methods with splines: an analysis of discrete Hodge–star operators*, arXiv preprint arXiv:2203.00620 (2022).
44. Dirk Pauly and Walter Zulehner, *On closed and exact Grad-grad-and div-Div-complexes, corresponding compact embeddings for tensor rotations, and a related decomposition result for biharmonic problems in 3D*, arXiv preprint arXiv:1609.05873 (2016).
45. ———, *The divDiv-complex and applications to biharmonic equations*, Applicable Analysis (2018), 1–52.
46. Hartmut Prautzsch, Wolfgang Boehm, and Marco Paluszny, *Bézier and B-spline techniques*, vol. 6, Springer, 2002.

47. Oliver Sander, *Conforming Finite Elements for* $H(\operatorname{sym}\operatorname{curl})$ *and* $H(\operatorname{dev}\operatorname{sym}\operatorname{curl})$, arXiv preprint arXiv:2104.12825 (2021).
48. Larry Schumaker, *Polynomial splines. in spline functions: Basic theory*, vol. 3, Cambridge University Press, 2007.
49. Yi Zhang, Varun Jain, Artur Palha, and Marc Gerritsma, *The Use of Dual B-Spline Representations for the Double de Rham Complex of Discrete Differential Forms*, Conference on Isogeometric Analysis and Applications, Springer, 2018, pp. 227–242.

MOX - Department of Mathematics, Politecnico di Milano. Via Bonardi 9, 20133 Milano.
Email address: `francesca.bonizzoni@polimi.it`

Mathematical Institute, University of Oxford, Andrew Wiles Building, Radcliffe Observatory Quarter, Oxford, OX2 6GG, UK.
Email address: `Kaibo.Hu@maths.ox.ac.uk`

Interdisciplinary Center for Scientific Computing (IWR), Heidelberg University, Im Neuenheimer Feld 205, 69120 Heidelberg, Germany
Email address: `kanschat@uni-heidelberg.de`

Mathematical Institute, University of Oxford, Andrew Wiles Building, Radcliffe Observatory Quarter, Oxford, OX2 6GG, UK.
Email address: `duygu.sap@maths.ox.ac.uk`

MOX Technical Reports, last issues

Dipartimento di Matematica
Politecnico di Milano, Via Bonardi 9 - 20133 Milano (Italy)

07/2023 Garcia-Contreras, G.; Còrcoles, J.; Ruiz-Cruz, J.A.; Oldoni, M; Gentili, G.G.; Micheletti, S.; Perotto, S.
Advanced Modeling of Rectangular Waveguide Devices with Smooth Profi les by Hierarchical Model Reduction

06/2023 Artoni, A.; Antonietti, P. F.; Mazzieri, I.; Parolini, N.; Rocchi, D.
A segregated finite volume - spectral element method for aeroacoustic problems

05/2023 Fumagalli, I.; Vergara, C.
Novel approaches for the numerical solution of fluid-structure interaction in the aorta

04/2023 Quarteroni, A.; Dede', L.; Regazzoni, F.; Vergara, C.
A mathematical model of the human heart suitable to address clinical problems

03/2023 Africa, P.C.; Perotto, S.; de Falco, C.
Scalable Recovery-based Adaptation on Quadtree Meshes for Advection-Diffusion-Reaction Problems

01/2023 Zingaro, A.; Bucelli, M.; Piersanti, R.; Regazzoni, F.; Dede', L.; Quarteroni, A.
An electromechanics-driven fluid dynamics model for the simulation of the whole human heart

02/2023 Boon, W. M.; Fumagalli, A.; Scotti, A.
Mixed and multipoint finite element methods for rotation-based poroelasticity

85/2022 Lurani Cernuschi , A.; Masci, C.; Corso, F.; Muccini, C.; Ceccarelli, D.; San Raffaele Hospital Galli, L.; Ieva, F.; Paganoni, A.M.; Castagna, A.
A neural network approach to survival analysis for modelling time to cardiovascular diseases in HIV patients with longitudinal observations

83/2022 Ciaramella, G.; Gander, M.; Mazzieri, I.
Unmapped tent pitching schemes by waveform relaxation

82/2022 Ciaramella, G.; Gander, M.; Van Criekingen, S.; Vanzan, T.
A PETSc Parallel Implementation of Substructured One- and Two-level Schwarz Methods